

## SI ISOTOPIC RATIOS IN MAINSTREAM PRESOLAR SiC GRAINS REVISITED

MARIA LUGARO<sup>1</sup>, ERNST ZINNER<sup>2</sup>, ROBERTO GALLINO<sup>3</sup>, SACHIKO AMARI<sup>2</sup>

1. Department of Mathematics, Monash University, Clayton 3168, Victoria, Australia

2. Laboratory for Space Physics and the Physics Department, Washington University, One Brookings Drive, St. Louis, MO 63130, USA

3. Dipartimento di Fisica Generale, Università di Torino, Via P. Giuria 1, I-10125 Torino, Italy

Submitted to the Astrophysical Journal

April 23, 1999

Revised July 19, 1999

*Draft version October 15, 2018*

## ABSTRACT

Although mainstream SiC grains, the major group of presolar SiC grains found in meteorites, are believed to have originated in the expanding envelope of asymptotic giant branch (AGB) stars during their late carbon-rich phases, their Si isotopic ratios show a distribution that cannot be explained by nucleosynthesis in this kind of stars. Previously, this distribution has been interpreted to be the result of contributions from many AGB stars of different ages whose initial Si isotopic ratios vary due to the Galactic chemical evolution of the Si isotopes. This paper presents a new interpretation based on local heterogeneities of the Si isotopes in the interstellar medium at the time the parent stars of the mainstream grains were born. Recently, several authors have presented inhomogeneous chemical evolution models of the Galactic disk in order to account for the well known evidence that F and G dwarfs of similar age show an intrinsic scatter in their elemental abundances.

First we report new calculations of the *s*-process nucleosynthesis of the Si and Ti isotopes in four AGB models (1.5, 3, and 5  $M_{\odot}$  with  $Z=0.02$ ; 3  $M_{\odot}$  with  $Z=0.006$ ). These calculations are based on the release of neutrons in the He intershell by the  $^{13}\text{C}$  source during the interpulse periods followed by a second small burst of neutrons released in the convective thermal pulse by the marginal activation of the  $^{22}\text{Ne}$  source. In the 1.5 and 3  $M_{\odot}$  models with solar metallicity the predicted shifts of the Si isotopic ratios in the stars' envelope are much smaller ( $< 30\text{ \%}$  for the  $^{29}\text{Si}/^{28}\text{Si}$  ratio and  $< 40\text{ \%}$  for the  $^{30}\text{Si}/^{28}\text{Si}$  ratio; the two ratios are normalized to solar) than the range observed in the mainstream grains (up to  $180\text{ \%}$ ). Isotopic shifts are of the same order as in the SiC grains for the 5  $M_{\odot}$  and  $Z=0.006$  models but the slope of the  $^{29}\text{Si}/^{28}\text{Si}$  vs.  $^{30}\text{Si}/^{28}\text{Si}$  correlation line is much smaller than that of the grains. We also show that none of the models can reproduce the correlations between the Ti and Si isotopic ratios measured in the mainstream grains as the result of *s*-process nucleosynthesis only.

To explain the distribution of the grains' Si isotopic compositions we constructed a simple Monte Carlo model in which contributions from classic Type Ia, Type Ia sub-Chandrasekhar, and Type II supernova (SN) models of different masses were admixed in a statistical way to material with a given Si isotopic composition. For four different starting compositions (average composition of the mainstream grains corrected for AGB contributions, solar composition, 100  $\text{\%}$  and 200  $\text{\%}$  deficits in  $^{29}\text{Si}$  and  $^{30}\text{Si}$  relative to solar) we show that, with the appropriate choice of two parameters, the distribution of the Si isotopic ratios in the mainstream grains can be successfully reproduced. The parameters to be adjusted are the total number of SN sources selected and the fraction of the material ejected from each SN that is mixed to the starting material. An upward adjustment of the supernova yield of  $^{29}\text{Si}$  relative to the other Si isotopes by a factor 1.5 was also introduced. Using current SN yields and Galactic chemical evolution models, this increase is necessary to achieve the Si isotopic ratios of the solar system.

If most mainstream SiC grains come from AGB stars that were born within a short time span, local heterogeneities must be the dominant cause of their Si isotopic variations. However, if AGB stars of different masses and therefore different ages contributed SiC to the solar system, the Si distribution of the mainstream grains reflect both the effect of Galactic chemical evolution of the Si isotopes and of isotopic heterogeneity at the time these stars were born.

*Subject headings:* dust, extinction – nuclear reactions, nucleosynthesis, abundances – AGB stars – supernovae: general

## 1. INTRODUCTION

Primitive meteorites contain presolar dust grains, grains that formed in stellar outflows and supernova (SN) ejecta and survived not only a long history as interstellar (IS) grains in the interstellar medium (ISM), but also the formation of the solar system and conditions in the meteorites' parent bodies (Anders & Zinner 1993; Ott 1993). The stellar origin of these grains is indicated by their isotopic compositions, which are completely different from those of material in the solar system and reflect

the compositions of their stellar sources. Their study in the laboratory provides information on stellar nucleosynthesis, Galactic chemical evolution (hereafter GCE), physical and chemical properties of stellar atmospheres and ejecta, and conditions in the early solar system (Bernatowicz & Zinner 1997; Zinner 1998).

The following types of presolar grains have been identified to date: diamond (Lewis et al. 1987), silicon carbide (SiC, carbonitride) (Bernatowicz et al. 1987), graphite (Amari et al.

1990), aluminum oxide ( $\text{Al}_2\text{O}_3$ , corundum), spinel ( $\text{MgAl}_2\text{O}_4$ ) (Hutcheon et al. 1994; Nittler et al. 1994) and silicon nitride ( $\text{Si}_3\text{N}_4$ ) (Nittler et al. 1995). In addition, graphite and SiC contain tiny subgrains of Ti carbide (graphite contains also Zr and Mo carbide) that were identified by transmission electron microscopy (Bernatowicz et al. 1991, 1996; Bernatowicz, Amari, & Lewis 1992). The carbonaceous phases diamond, SiC and graphite were discovered because they carry isotopically anomalous noble gases (Tang & Anders 1988a; Lewis, Amari, & Anders 1990, 1994; Huss & Lewis 1994a,b; Amari, Lewis, & Anders 1995a); they can be extracted from meteorites in almost pure form by chemical and physical processing (Tang et al. 1988; Amari, Lewis, & Anders 1994). This results in relatively large amounts (micrograms) of samples that can be analyzed in great detail. In contrast, presolar corundum and silicon nitride have been discovered by ion microprobe isotopic measurements of individual grains from chemically resistant residues and only a limited number of grains ( $\sim 100$  for corundum) have been measured to date.

Silicon carbide, graphite, corundum, and  $\text{Si}_3\text{N}_4$  grains are large enough (up to several  $\mu\text{m}$  in diameter for corundum and  $\text{Si}_3\text{N}_4$ , up to  $> 10 \mu\text{m}$  for SiC and graphite) to be analyzed individually for their elemental and isotopic compositions. The ion microprobe makes it possible to measure isotopic ratios of major and some minor elements in single grains down to  $\sim 0.5 \mu\text{m}$  in diameter (e.g., Hoppe et al. 1994, 1995; Huss, Hutcheon, & Wasserburg 1997; Travaglio et al. 1999). Ion microprobe isotopic measurements have been made for C, N, O, Mg, Si, K, Ca, and Ti on many (for the major elements on thousands of) grains (see, e.g., Zinner 1998). Single grain isotopic measurements, albeit on a limited number of grains, have also been made for Zr, Mo, and Sr by resonance ionization mass spectrometry (Nicolussi et al. 1997, 1998a,b,c; Davis et al. 1999; Pellin et al. 1999); and for He and Ne by laser extraction and noble gas mass spectrometry (Nichols et al. 1991, 1994; Kehm et al. 1996). Diamonds, instead, are too small ( $\sim 2 \text{ nm}$ ) for single grain analysis and isotopic measurements have been made on “bulk samples”, collections of many grains. Bulk analyses have also been made in SiC and graphite of the noble gases (Lewis et al. 1994; Amari et al. 1995a) and of trace elements such as Sr, Ba, Nd, Sm, and Dy in SiC (see, e.g., Anders & Zinner 1993; Hoppe & Ott 1997; Zinner 1998).

Based on their isotopic compositions, several stellar sources have been identified for presolar grains. Most corundum grains are believed to have originated in low-mass red giant (RG) and asymptotic giant branch (AGB) stars. This identification rests on the O isotopic ratios and inferred  $^{26}\text{Al}/^{27}\text{Al}$  ratios (Huss et al. 1994; Nittler et al. 1997; Nittler 1997; Choi et al. 1998; Nittler & Alexander 1999a). Low-density graphite grains, a subtype of SiC grains termed X grains, and  $\text{Si}_3\text{N}_4$  grains have isotopic signatures indicative of a SN origin (Nittler et al. 1995; Travaglio et al. 1999). A SN origin has also been proposed for a few corundum grains (Nittler et al. 1998; Choi et al. 1998). In addition, a few rare SiC grains with large  $^{30}\text{Si}$  excesses and low  $^{12}\text{C}/^{13}\text{C}$  and  $^{14}\text{N}/^{15}\text{N}$  ratios are possibly of a nova origin (Gao & Nittler 1997).

Most SiC grains, in particular the “mainstream” component, which accounts for  $\sim 93\%$  of all SiC (Hoppe et al. 1994; Hoppe & Ott 1997), are believed to come from carbon stars, thermally pulsing (TP) AGB stars during late stages of their evolution. The best evidence for such an origin are the *s*-process (slow neutron capture process) isotopic patterns displayed by the heavy elements Kr, Sr, Zr, Mo, Xe, Ba, Nd, and Sm (Lewis

et al. 1994; Hoppe & Ott 1997; Gallino, Raiteri, & Busso 1993; Gallino, Busso, & Lugardo 1997; Nicolussi et al. 1997, 1998a; Pellin et al. 1999) and the presence of Ne-E(H), almost pure  $^{22}\text{Ne}$  (Lewis et al. 1990, 1994; Gallino et al. 1990). The C and N isotopic compositions as well as  $^{26}\text{Al}/^{27}\text{Al}$  ratios of individual mainstream SiC grains are by and large consistent with a carbon star origin (Hoppe et al. 1994; Huss et al. 1997; Hoppe & Ott 1997).

In contrast to C, N, Ne, Al and the heavy elements, the variations in the Si (and Ti) isotopic ratios measured in single mainstream grains cannot be explained in terms of nucleosynthesis in AGB stars (Gallino et al. 1990, 1994; Brown & Clayton 1992a). They have been interpreted to indicate that many stellar sources (Clayton et al. 1991; Alexander 1993), whose initial compositions vary because of GCE, contributed SiC grains to the solar system (Gallino et al. 1994; Timmes & Clayton 1996; Clayton & Timmes 1997a). However, a fundamental problem with this interpretation is the fact that the metallicity implied by the Si isotopic compositions of the mainstream grains is higher than that of the sun. This would mean that the grains are younger than the solar system. A solution to this puzzle has been proposed by Clayton (1997) who considered the possibility that the sun and the AGB stars that were the sources of the mainstream grains did not originate in the same Galactic region but changed their positions because of Galactic diffusion. Alexander & Nittler (1999), on the other hand, used the Si and Ti isotopic compositions of the mainstream grains themselves (Figs. 3 and 4) to infer the metallicity of the ISM at the time of solar system formation. From this exercise they concluded that the sun has an atypical Si isotopic composition.

In this paper we will revisit the Si isotopic compositions of the mainstream SiC grains. In §2 we will first describe the isotopic properties of these grains in greater detail, discuss their AGB origin, and review previous attempts to understand their Si isotopic ratios. After presenting new calculations for the nucleosynthesis of Si (and Ti) in AGB stars (§3), we will present a new approach to the problems of the distribution of Si isotopic ratios (§4): instead of assuming an average monotonic relationship of metallicity with time in the Galaxy, we investigate how heterogeneities in the Si isotopic ratios could result from fluctuations in the contributions from various types of nucleosynthetic sources to the low-mass stars that, in their AGB phase, produced the SiC grains. Preliminary accounts can be found in Lugardo et al. (1999a,b).

Galactic chemical evolution models of the Galactic disk that, although in different ways, deal with compositional inhomogeneities in the ISM have previously been presented by Malinie et al. (1993), Wilmes & Köppen (1995), Copi (1997) and van den Hoek & de Jong (1997). We will show that our approach is consistent with the results obtained by inhomogeneous GCE models, which, however, did not address the evolution of isotopic compositions.

## 2. METEORITIC SiC, THE MAINSTREAM COMPONENT AND THE Si ISOTOPE PUZZLE

Among all presolar grains, SiC has been most widely studied because it is relatively abundant (6 ppm in the Murchison and in similar primitive meteorites) and is present in various classes of meteorites (Huss & Lewis 1995). Ion microprobe isotopic analyses of single grains have revealed several distinct classes. This is shown in Figs. 1 and 2, which display the C, N, and Si isotopic ratios. For historical reasons the Si isotopic ratios are expressed as  $\delta$ -values, deviations in permil ( $^{\circ}/\text{oo}$ ) from the solar

isotopic ratios of  $(^{29}\text{Si}/^{28}\text{Si})_{\odot} = 0.0506331$  and  $(^{30}\text{Si}/^{28}\text{Si})_{\odot} = 0.0334744$  (Zinner, Tang, & Anders 1989):

$$\delta^{29}\text{Si}/^{28}\text{Si} = [(^{29}\text{Si}/^{28}\text{Si})_{\text{meas}} / (^{29}\text{Si}/^{28}\text{Si})_{\odot} - 1] \times 1000,$$

$$\delta^{30}\text{Si}/^{28}\text{Si} = [(^{30}\text{Si}/^{28}\text{Si})_{\text{meas}} / (^{30}\text{Si}/^{28}\text{Si})_{\odot} - 1] \times 1000.$$

According to their C, N and Si isotopic compositions five different groups of grains can be distinguished and these groups are indicated in the figures. Also indicated in the figures are the abundances of the different groups. By far the most common grains are the mainstream grains. It should be noted that the frequency distributions of grains in the plots of Figs. 1 and 2 do not correspond to their abundances in meteorites, but that rare grain types, located by automatic imaging in the ion probe (Nittler et al. 1995; Amari et al. 1996) are over-represented. An additional grain with extreme  $^{29}\text{Si}$  and  $^{30}\text{Si}$  excesses has been found (Amari, Zinner, & Lewis 1999); its composition ( $\delta^{29}\text{Si}/^{28}\text{Si} = 2678 \text{ ‰}$ ,  $\delta^{30}\text{Si}/^{28}\text{Si} = 3287 \text{ ‰}$ ) lies outside the boundaries of the plot in Fig. 2.

The possible stellar sources of the different groups of SiC grains have been discussed elsewhere (e.g., Zinner 1998). Here we wish to concentrate on grains of the mainstream component (Hoppe et al. 1994; Hoppe & Ott 1997). Their  $^{12}\text{C}/^{13}\text{C}$  ratios lie between 15 and 100 and their  $^{14}\text{N}/^{15}\text{N}$  ratios between the solar ratio of 272 and 10,000 (Fig. 1). Their Si isotopic ratios plot along a line of slope 1.31 in a  $\delta^{29}\text{Si}/^{28}\text{Si}$  vs.  $\delta^{30}\text{Si}/^{28}\text{Si}$  3-isotope plot (Fig. 3). Most grains show large  $^{26}\text{Mg}$  excesses attributed to the presence of  $^{26}\text{Al}$  ( $T_{1/2} = 7 \times 10^5 \text{ yr}$ ), now extinct, at the time of their formation. Inferred  $^{26}\text{Al}/^{27}\text{Al}$  ratios range up to  $10^{-2}$  (Hoppe et al. 1994; Huss et al. 1997). Much more limited isotopic data exist for Ti. In Fig. 4 the measurements by Hoppe et al. (1994) and Alexander & Nittler (1999) are plotted as  $\delta^4\text{Ti}/^{48}\text{Ti}$  values against the  $\delta^{29}\text{Si}/^{28}\text{Si}$  values of these grains. The correlation between the Ti ratios, especially  $\delta^{46}\text{Ti}/^{48}\text{Ti}$ , and the Si isotopic ratios has already been noticed by Hoppe et al. (1994).

There are many pieces of evidence that indicate that mainstream SiC grains come from carbon stars. Carbon stars are TP-AGB stars whose spectra are dominated by lines of C compounds such as  $\text{C}_2$ ,  $\text{CH}$ , and  $\text{CN}$ , indicating that  $\text{C} > \text{O}$  in their envelopes (Secchi 1868). They become C-rich because of the recurrent third dredge up (TDU) episodes mixing with the envelope newly synthesized  $^{12}\text{C}$  from the He shell where it is produced by the triple- $\alpha$  reaction (Iben & Renzini 1983). For high-temperature carbonaceous phases, such as SiC, to condense from a cooling gas the condition  $\text{C} > \text{O}$  has to be satisfied (Larimer & Bartholomay 1979; Sharp & Wasserburg 1995; Lodders & Fegley 1997a). Carbon stars experience substantial mass loss by stellar winds and have extended atmospheres with temperatures of 1500 - 2000 K, at which SiC is expected to condense. In fact, carbon stars are observed to have circumstellar dust shells that show the  $11.3 \mu\text{m}$  emission feature of SiC (Cohen 1984; Little-Marenin 1986; Martin & Rogers 1987; Speck, Barlow, & Skinner 1997). Recently, Clayton, Liu, & Dalgarno (1999) proposed that in a SN environment with high levels of ionizing  $\gamma$ -rays carbon dust can condense from a gas of  $\text{O} > \text{C}$ . However, even if this should be possible, it would not apply to the expanding atmospheres of carbon stars. In contrast to such atmospheres, the solar system is characterized by  $\text{O} > \text{C}$  and phases such as SiC are not believed to be able to form under these conditions. This apparently is the reason why all SiC grains found in primitive meteorites are of presolar origin according to their isotopic compositions. This is in marked contrast to presolar corundum grains, which make up only a small

fraction ( $\sim 1\%$ ) of all meteoritic corundum grains.

Isotopic compositions of presolar grains are the most diagnostic indicators of their stellar sources. As already mentioned in §1, the *s*-process patterns of the heavy elements exhibited by mainstream SiC grains constitute the most convincing argument for their origin in carbon stars, which are the major source of the *s*-process elements in the Galaxy. The envelopes of these stars show large enhancements of typical *s*-elements such as Sr, Y, Zr, Ba, La, Ce, and Nd (Smith & Lambert 1990). In SiC grains *s*-process patterns are seen in the elements Kr, Xe, Sr, Ba, Nd, Sm, and Dy (Lewis et al. 1990, 1994; Ott & Begemann 1990a,b; Prombo et al. 1993; Richter, Ott, & Begemann 1993, 1994; Zinner, Amari, & Lewis 1991; Podosek et al. 1999), which have been measured in bulk samples. Although these samples were collections of all SiC grain types, there is little doubt that the isotopic results must have been dominated by contributions of mainstream grains.

In addition, isotopic analyses of Sr, Zr, and Mo by resonance ionization mass spectrometry (RIMS) have been made on a limited number of single SiC grains. Although most of these measurements were made on SiC grains for which no C and Si isotopic data had been obtained (Nicolussi et al. 1997, 1998a,b), for statistical reasons essentially all of these grains must have been mainstream grains. They display characteristic *s*-process patterns with large depletions in the *p*-only isotopes  $^{84}\text{Sr}$ ,  $^{92}\text{Mo}$ , and  $^{94}\text{Mo}$ , and in the *r*-only isotope  $^{100}\text{Mo}$ . Large depletions are also seen in  $^{96}\text{Zr}$ , indicating that neutron densities in the stellar sources of these grains must have been low, compatible with  $^{13}\text{C}$  being the major neutron source in AGB stars (Gallino et al. 1998a). The depletions in  $^{96}\text{Zr}$  are consistent with isotopic abundance data obtained by spectroscopic observations of the ZrO bandheads in AGB star envelopes (Lambert et al. 1995). Recent RIMS analysis of Mo in SiC grains that had been identified as mainstream grains on the basis of their C, N, and Si isotopic ratios confirmed that mainstream grains indeed carry *s*-process signatures in this element (Pellin et al. 1999). Gallino et al. (1997) could successfully reproduce the measured *s*-process compositions of the heavy elements in mainstream SiC grains with models of low-mass AGB stars of close-to-solar metallicity, in which neutrons are primarily produced by the  $^{13}\text{C}$  source during the radiative interpulse period. In addition to the isotopic patterns of the heavy elements, the large overabundances of refractory *s*-process elements such as Zr, Y, Ba, and Nd in single SiC grains (Amari et al. 1995b) are further evidence for an AGB-star origin (Lodders & Fegley 1995, 1997a,b, 1998).

Evidence for a carbon star origin is also obtained from the light elements. It should be noted that as far as neutron-capture nucleosynthesis is concerned, because of their large abundance the light elements (elements lighter than Fe) in AGB stars are considered to be neutron poisons for the synthesis of the heavy elements. However, because of their relatively small cross sections, they are only marginally affected by neutron capture. Elements up to Mg are also affected by charged particle reactions with H and He. The most important light-element signature of SiC is the Ne isotopic composition, which is dominated by  $^{22}\text{Ne}$  (Lewis et al. 1990, 1994). In fact, it has been the presence of this Ne component, Ne-E(H), that, together with the so-called Xe-S component (Srinivasan & Anders 1978; Clayton & Ward 1978) led to the isolation of presolar SiC (Tang & Anders 1988a). Gallino et al. (1990, 1994) showed that Ne-E(H) matches the predicted isotopic composition of Ne in the He shell of AGB stars. Almost all initial CNO nuclei are first

converted to  $^{14}\text{N}$  during shell H burning and then to  $^{22}\text{Ne}$  via the chain  $^{14}\text{N}(\alpha, \gamma)^{18}\text{F}(\beta^+ \nu)^{18}\text{O}(\alpha, \gamma)^{22}\text{Ne}$  in the He shell during thermal pulses. Another piece of evidence is obtained from the distribution of the  $^{12}\text{C}/^{13}\text{C}$  ratios in mainstream grains that is very similar to that measured astronomically in carbon stars (Dominy & Wallerstein 1987; Smith & Lambert 1990; see also Fig. 14 in Anders & Zinner 1993).

The ranges of  $^{12}\text{C}/^{13}\text{C}$  and  $^{14}\text{N}/^{15}\text{N}$  ratios measured in mainstream grains roughly agree with the ranges predicted by theoretical models of AGB stars. Proton captures occurring in the deep envelope during the main sequence phase followed by first (and second) dredge-up as well as shell He burning and the TDU during the TP-AGB phase affect the C and N isotopes in the envelope.  $^{12}\text{C}/^{13}\text{C}$  ratios predicted by canonical stellar evolution models range from  $\sim 20$  at first dredge-up in the RG phase to  $\sim 300$  in the late TP-AGB phases (Iben 1977a; Bazan 1991; Gallino et al. 1994). Predicted  $^{14}\text{N}/^{15}\text{N}$  ratios are 600 - 1,600 (Becker & Iben 1979; El Eid 1994), falling short of the range observed in the grains. However, the assumption of deep mixing (“cool bottom processing” or CBP) of envelope material to deep hot regions in  $M \lesssim 2.5 M_\odot$  stars during their RG and AGB phases (Charbonnel 1995; Wasserburg, Boothroyd, & Sackmann 1995; see also Langer et al. 1999a for rotationally induced mixing) results in partial H burning, with higher  $^{14}\text{N}/^{15}\text{N}$  and lower  $^{12}\text{C}/^{13}\text{C}$  ratios in the envelope than in canonical models (see also Huss et al. 1997). As a matter of fact, CBP mechanisms have been introduced to explain the observed  $^{12}\text{C}/^{13}\text{C}$  ratios in RG stars of low mass (Gilroy 1989; Gilroy & Brown 1991; Pilachowski et al. 1997), which are lower than those predicted by canonical models.

In contrast to the heavy elements, and the light elements C, N, Ne and Al, the Si isotopic ratios of mainstream SiC grains cannot be explained by nuclear processes taking place in a single star. In Fig. 3 we plotted the Si isotopic data measured in SiC grains from three different size fractions isolated from the Murchison carbonaceous (CM2) meteorite (Hoppe et al. 1994, 1996a) and data from the Orgueil (CI) meteorite (Huss et al. 1997). The three Murchison size fractions are KJE (0.5 - 0.8  $\mu\text{m}$  in diameter), KJG (1.5 - 3  $\mu\text{m}$ ), and KJH (3 - 5  $\mu\text{m}$ ) (Amari et al. 1994). Of the smallest Murchison grain size fraction KJE we plotted only data points with errors smaller than 15 ‰. The distributions of Si isotopic ratios measured in SiC grains from other meteorites are very similar to that shown in Fig. 3 (Alexander 1993; Huss, Fahey, & Wasserburg 1995; Gao et al. 1995). Also plotted in Fig. 3 is the correlation line obtained from a fit to the grain data. This line, which does not go through the solar composition but passes slightly to the right of it, has a slope of 1.31 and an intercept of the ordinate at  $\delta^{29}\text{Si}/^{28}\text{Si}_{\text{int}} = -15.9$  ‰, a little different from the parameters determined from the KJG and KJH dataset only (Hoppe et al. 1994).

There have been various attempts to explain the Si isotopic distribution of the mainstream SiC grains. Zinner et al. (1989) already realized that the scatter in the Si isotopic ratios indicate several stellar sources. Stone et al. (1991) first noticed the correlation line of Si isotopic ratios in SiC grains from Orgueil and proposed an origin in a single AGB star with mixing of two components but they did not address the question of how the end components could be generated by nucleosynthetic processes in a single star. The only nuclear reactions in AGB stars that are believed to substantially affect the Si isotopes are neutron captures in the He shell. However, it has been determined early on (Gallino et al. 1990; Obradovic et al. 1991; Brown & Clayton 1992b), and will be seen in more detail in the §3, that

neutron captures shift the Si isotopic ratios along a line with a slope that varies, depending on mass and metallicity, from 0.35 to 0.75 in a  $\delta^{29}\text{Si}/^{28}\text{Si}$  vs.  $\delta^{30}\text{Si}/^{28}\text{Si}$  3-isotope plot. Furthermore, in low-mass AGB stars of close-to-solar metallicity predicted shifts of envelope material are only on the order of 20 ‰, an order of magnitude less than the range seen in mainstream grains. Nuclear processes in a single AGB star therefore cannot produce the mainstream distribution and this led to the conclusion that several stars with varying initial Si isotopic compositions must have contributed SiC grains to the solar system (Clayton et al. 1991; Alexander 1993). The situation is similar for Ti. It should be emphasized that there is a fundamental qualitative difference between the isotopic compositions of C, N, Ne, and the heavy elements, and those of Si and Ti. While the former are dominated by RG and AGB nucleosynthesis, the effect of stellar nucleosynthesis on the Si and Ti ratios is relatively small and cannot explain the compositions observed in grains; the presence of an extra component has to be invoked.

Brown & Clayton (1992b, 1993) proposed a single-star model by considering Mg burning at elevated temperatures in the He-burning shell. In this model  $(\alpha, n)$  reactions on Mg in a  $5.5 M_\odot$  AGB star produce a neutron-rich Si isotopic composition at the far end of the mainstream correlation line. Mixing with the original, close to solar, composition in the envelope combined with variable mass loss from this star could lead to the observed distribution. However, to accomplish this, the temperature in the He shell has to be raised by 10% above that produced by the standard AGB models (Iben 1977b). This leads to serious problems with other processes and with the general question of energy generation and stellar structure. Moreover, the Ti isotopic variations and especially the correlation with the Si isotopic ratios (Fig. 4) cannot be explained in this way because the temperatures required for Mg burning in the He shell do not affect at all the Ti isotopes, nor would the *s*-process isotopic signatures be compatible with such a situation.

This leaves variations in the initial Si isotopic compositions of the AGB stars that contributed SiC grains to the solar system as the most likely explanation for the Si isotope distribution of mainstream grains. Variations of the initial Si compositions in turn are expected as the result of GCE. Low-mass stars, which became AGB stars at the end of their evolution and contributed grains to the protosolar nebula, are likely to have been born at different times before solar system formation and thus reflect the isotopic composition of the Galaxy in different earlier epochs. An explanation of the Si isotopic compositions in mainstream grains thus requires an understanding of the evolution of the Si isotopic ratios throughout Galactic history.

Gallino et al. (1994) approached this problem by assuming that  $^{29}\text{Si}$  and  $^{30}\text{Si}$  are mostly primary isotopes that are produced by SNe of Type II, together with a major fraction of  $^{28}\text{Si}$ , and that substantial contributions to Galactic Si in the form of almost pure  $^{28}\text{Si}$  from SNe of Type Ia late in Galactic history determine the Si isotopic evolution reflected by the grains. These authors also advanced a tentative interpretation of the Ti isotopes. They noticed the correlation between the Ti and Si isotopic compositions (Fig. 4) and concluded that, as for Si, neutron-capture nucleosynthesis cannot explain the Ti isotopes nor the correlation with Si and they would have to be interpreted within the framework of the chemical evolution of the Galaxy.

Timmes & Clayton (1996) and Clayton & Timmes (1997a,b) constructed a detailed model of the Galactic history of the Si isotopes that is based on the GCE model of Timmes, Woosley & Weaver (1995). The SN production yields were obtained from

the Type II SN models of Woosley & Weaver (1995, henceforth WW95) and from the popular W7 Type Ia SN model by Thielemann, Nomoto, & Yokoi (1986). According to the WW95 models,  $^{29}\text{Si}$  and  $^{30}\text{Si}$  in Galactic disk stars are predominantly secondary isotopes, i.e. their production in massive Type II SNe increases with increasing metallicity, since it requires the prior presence of primary isotopes such as  $^{12}\text{C}$ ,  $^{14}\text{N}$  and  $^{16}\text{O}$ . As a consequence, early SNI $\text{Ie}$  produced mostly pure  $^{28}\text{Si}$ , whereas later SNI $\text{Ie}$  added more and more  $^{29}\text{Si}$  and  $^{30}\text{Si}$  to the ISM. This resulted in a continuous increase of the  $^{29}\text{Si}/^{28}\text{Si}$  and  $^{30}\text{Si}/^{28}\text{Si}$  ratios throughout Galactic history and the distribution of the grains' Si isotopic ratios apparently reflects this change. According to the Timmes & Clayton model, the spread in the isotopic compositions of the mainstream grains corresponds to variations in the birth dates of their parent stars. Specifically, the birth dates of the parents stars range over  $\sim 5$  Gyr (see Fig. 6 in Timmes & Clayton 1996).

However, this model suffers from a fundamental problem. Because most mainstream grains have  $^{29}\text{Si}/^{28}\text{Si}$  and  $^{30}\text{Si}/^{28}\text{Si}$  ratios that are larger than those of the solar system (Fig. 3), they are inferred to be younger than the sun. This absurd corollary of the model led Clayton (1997) to consider the possibility that the mainstream grains originated from stars that were born at different Galactic radii than the sun. Indeed, according to Wielen, Fuchs, & Dettbarn (1996), scattering by massive molecular clouds may lead to the diffusion of those stars from central metal-rich regions of the Galaxy (for which higher  $^{29}\text{Si}/^{28}\text{Si}$  and  $^{30}\text{Si}/^{28}\text{Si}$  ratios are predicted than those in the present solar neighborhood) to the region where they, once they became AGB stars, shed their SiC grains into the protosolar cloud. Alexander & Nittler (1999) took a different approach to resolve the paradox that the grains are apparently younger than the sun. They fitted the Si and Ti isotopic compositions of the mainstream grains to contributions from nucleosynthesis in the parent AGB stars and the stars' original isotopic compositions. However, in contrast to the Timmes & Clayton (1996) model, they tried to determine the evolution of the Si and Ti isotopes from the grain data themselves. From this fit they concluded that most mainstream grains do not come from stars with higher than solar metallicities but that the sun has an atypical Si isotopic composition.

Common to the GCE models listed above is that they predict a monotonic relationship between the Si isotopic composition and Galactic time for the ISM at a given Galactic radius. In other words, a given age of the Galaxy or, if different Galactic radii are considered, a given function of age and Galactic radius corresponds to a given isotopic composition (this functional relationship is implied in the Clayton & Timmes (1997a) model but has never been explicitly worked out).

However, one has to consider that the Si isotopic composition of the Galaxy, and in particular that of different regions where individual low-mass stars are born, evolves as the result of contributions from discrete stellar sources, mostly SNe. It is unlikely that these discrete contributions are instantly mixed with preexisting material so that the isotopic compositions of large Galactic regions are completely homogenized. The work of Edvardsson et al. (1993) and others has shown that stars from any given Galactic epoch and Galactic radius display a considerable spread in metallicity and, more generally, in elemental abundances. Numerous attempts have been made to explain these observations: stellar orbital diffusion, chemical condensation processes and/or thermal diffusion in stellar atmospheres, incomplete mixing of stellar ejecta, sequential stel-

lar enrichment and local infall of metal-deficient gas (see van den Hoek & de Jong 1997 for review and discussion of these different attempts).

The study of meteorites provided ample evidence that the protosolar nebula was isotopically not homogenized. In addition to the survival of pristine stardust, isotopic anomalies are found in material that apparently was processed in the solar nebula (see, e.g., Clayton, Hinton, & Davis 1988; Lee 1988; Wasserburg 1987). Examples include  $^{16}\text{O}$  excesses (up to 5%) and large deficits and excesses of the n-rich isotopes of the Fe-peak elements such as  $^{48}\text{Ca}$  and  $^{50}\text{Ti}$  in refractory inclusions. These anomalies indicate the survival of isotopic signatures from different nucleosynthetic reservoirs. Another indication of local isotopic heterogeneity comes from the value of the  $^{17}\text{O}/^{18}\text{O}$  ratio, which is 5.26 in the solar system but  $3.65 \pm 0.15$  in diverse molecular clouds (Penzias 1981; Wannier 1989; Henkel & Mauersberg 1993, see also discussion concerning the  $^{14}\text{N}/^{15}\text{N}$  ratio by Chin et al. 1999).

We therefore want to explore to what extent the Si isotopic spread of mainstream SiC grains can be explained by local heterogeneities in the regions from which the low-mass parent stars of the grains originally formed. Before doing this we will examine in more detail the nucleosynthesis of the Si and Ti isotopes in AGB stars. However, because of the largely uncertain astrophysical origin of all Ti isotopes (see Timmes et al. 1995; Woosley 1996; Woosley et al. 1997), the situation concerning the Ti isotopes in presolar SiC grains and their interpretation in terms of SN contributions and GCE is a complicated issue in itself. It will be treated in a separate paper.

### 3. NUCLEOSYNTHESIS OF THE SI AND TI ISOTOPES IN AGB STARS

During all the evolutionary phases of low-mass stars ( $M < 10 M_{\odot}$ ) the maximum temperature in the inner regions never reaches high enough values to allow the burning of any element heavier than He. Consequently, only the production of  $^{12}\text{C}$  and of  $^{16}\text{O}$  from initial H or He nuclei is possible and, in particular, there are no charged-particle interactions that involve the nucleosynthesis of Si and Ti. The initial isotopic compositions of these elements can be nevertheless modified by slow neutron capture (the *s* process), which occurs in the tiny region between the H shell and the He shell (hereafter He intershell) during the AGB phase.

According to the AGB models of low-mass ( $M = 1.5 - 3 M_{\odot}$ ) stars with metallicities in the range from half solar to solar obtained with the FRANEC code and discussed in detail by Straniero et al. (1997) and Gallino et al. (1998a), neutrons are released in the He intershell by two different sources,  $^{13}\text{C}$  and  $^{22}\text{Ne}$ . The maximum temperature achieved during the recurrent thermal instabilities (or thermal pulses: TP) of the He shell is not high enough to consume  $^{22}\text{Ne}$  to an appreciable extent, so that the  $^{13}\text{C}$  source has to play the major role. However, the number of  $^{13}\text{C}$  nuclei left behind by the H-burning shell is too small to account for the *s*-element enhancements observed in carbon stars. A special mechanism has to be invoked in order to build up a sufficient amount of  $^{13}\text{C}$  in the He intershell. In AGB stars of mass  $M \gtrsim 1.5 M_{\odot}$ , after a limited number of thermal pulses, soon after the quenching of a given instability, the convective envelope penetrates into the top layers of the He intershell and mixes with the envelope material enriched in  $^{12}\text{C}$  and *s*-process elements. This TDU phenomenon leaves a sharp H/He discontinuity, where some kind of hydrodynamical mixing, possibly driven by rotation, occurs (Herwig et al. 1997; Singh, Roxburgh, & Chan 1998; Langer et al. 1999a,b).

In these conditions, a small amount of protons penetrates from the envelope into the He intershell (see Gallino et al. 1998a for discussion). At H reignition, these protons are captured by the abundant  $^{12}\text{C}$  present in the intershell as a consequence of partial He burning that occurred during the previous thermal instability. Consequently, a so-called  $^{13}\text{C}$  pocket is formed in a small region at the top of the He intershell. Before the onset of the next pulse, the progressive compression and heating of these layers cause all  $^{13}\text{C}$  to burn radiatively in the interpulse period via the  $^{13}\text{C}(\alpha, n)^{16}\text{O}$  reaction, at a temperature of around 8 keV. The neutron exposure, or time integrated neutron flux  $\delta\tau = \int N_n v_{th} dt$ , experienced during the interpulse period may reach quite a high value,  $\delta\tau_1(8\text{keV})$  of up to  $0.4 \text{ mbarn}^{-1}$ , depending on the initial amount of  $^{13}\text{C}$ . The maximum neutron density in this radiative phase remains low:  $N_{n,max} \sim 10^7 \text{ n/cm}^3$ .

The material that experienced neutron captures in the  $^{13}\text{C}$  pocket is engulfed and diluted ( $\sim 1/20$ ) by the next growing convective thermal pulse, which extends over almost the whole He intershell, and is mixed with material already *s*-processed during the previous pulses, together with ashes of the H-burning shell. Among them are Si and Ti in their initial abundances. For advanced pulses, the overlapping factor between subsequent pulses becomes  $r \approx 0.4$  and the mass of the convective pulse is slightly smaller than  $10^{-2} M_\odot$  (Gallino et al. 1998a). A small neutron burst, at around 23 keV, is released in convective thermal pulses, during the latest phases of the AGB evolution, when the bottom temperature in the He shell is sufficiently high to marginally activate the  $^{22}\text{Ne}(\alpha, n)^{25}\text{Mg}$  reaction. The  $^{22}\text{Ne}$  is provided by the  $^{14}\text{N}(\alpha, \gamma)^{18}\text{F}(\beta^+ \nu)^{18}\text{O}(\alpha, \gamma)^{22}\text{Ne}$  chain starting from  $^{14}\text{N}$  present in the ashes of H burning. Some extra  $^{14}\text{N}$  derives from primary  $^{12}\text{C}$  that is dredged up into the envelope and partly converted to  $^{14}\text{N}$  by H-shell burning. The neutron exposure provided by the  $^{22}\text{Ne}$  neutron source during the thermal pulse is low, reaching at most  $\delta\tau_2(23\text{keV}) = 0.03 \text{ mbarn}^{-1}$ . However, the peak neutron density can reach  $10^{10} \text{ n/cm}^3$ .

Exposure to the two neutron fluxes is repeated through the pulses with TDU. The  $^{13}\text{C}$ -pocket features are kept constant pulse after pulse, while the small neutron exposure from the  $^{22}\text{Ne}$  neutron source during thermal pulses increases with pulse number, reflecting the slight increase of the strength of the thermal instability with core mass.

We have performed new calculations for the nucleosynthesis due to neutron capture in AGB stars. These calculations are based on the stellar models and the nuclear network described in detail by Gallino et al. (1998a). We want to follow here in particular the modifications of the Si and Ti isotope abundances arising by neutron capture in the intershell region during the neutron fluences in the  $^{13}\text{C}$  pocket and in the thermal pulses. Then we will follow the isotopic compositions of Si and Ti in the envelope as they are modified during the whole TP-AGB phase by the mixing of He intershell material due to TDU episodes. The envelope itself is progressively eroded by stellar winds and by the growth of the H-burning shell.

In Table 1 the Maxwellian averaged neutron capture cross sections (in the form of  $\sigma_{code} = \langle \sigma v \rangle / v_{th}(30\text{keV})$ , expressed in mbarn) are listed for selected isotopes. Values are reported for the two typical temperatures (8 keV and 23 keV) at which neutrons are released by the  $^{13}\text{C}$  and by the  $^{22}\text{Ne}$  neutron source, and for the standard temperature of 30 keV at which these cross sections are currently given in the literature. The quoted values have been taken from the compilation by Beer, Voss, & Winters (1992), with three exceptions:  $^{28}\text{Si}$ , for which a renormal-

ization to the 30 keV recommended value of Bao & Käppeler (1987) has been considered (Beer 1992, private communication),  $^{150}\text{Sm}$ , from Wissak et al. (1993), and the  $^{33}\text{S}(\text{n}, \alpha)^{30}\text{Si}$  cross section from Schatz et al. (1995). The use of  $\sigma_{code}$  demonstrates how the cross section at any given energy departs from the usual  $1/v$  rule. For a perfect  $1/v$  dependence,  $\sigma_{code}$  at different  $kT$  values should remain constant. In reality, with the exception of  $^{49}\text{Ti}$ , strong departures from this rule are shown by all Si and Ti isotopes. The  $^{30}\text{Si}$  abundance resulting from a given neutron exposure is strongly dependent on the reaction rate of  $^{32}\text{S}(\text{n}, \gamma)^{33}\text{S}$ , where  $^{33}\text{S}$  is subsequently quickly transformed to  $^{30}\text{Si}$  via  $^{33}\text{S}(\text{n}, \alpha)^{30}\text{Si}$ .

The neutron capture cross sections of two typical heavy *s*-only nuclei,  $^{100}\text{Ru}$  and  $^{150}\text{Sm}$ , have also been included in Table 1 in order to show that Si and Ti (this is also true for all other elements lighter than Fe) are not as much affected by neutron capture as the heavier elements. The neutron capture cross sections of light elements are much smaller (by as much as three orders of magnitude) than those of typical heavy isotopes. However, because of their large initial abundances, isotopes lighter than  $^{56}\text{Fe}$  act as important neutron poisons for the build-up of the heavy elements. In the last column, the relative uncertainties of the 30 keV cross sections are reported. The cross sections of all Si and Ti isotopes still suffer from large uncertainties, around 10%, whereas for many heavy isotopes recent experiments have achieved a precision of the order of 1% (see Käppeler 1999).

Table 2 shows the production factors with respect to solar of the Si and Ti isotopes, as well as that of two *s*-only nuclei  $^{100}\text{Ru}$  and  $^{150}\text{Sm}$ , in the He intershell at different phases of the 15<sup>th</sup> thermal pulse for an AGB star of  $1.5 M_\odot$  and solar metallicity, with the standard choice of the  $^{13}\text{C}$  pocket (case ST of Gallino et al 1998a). Columns 2 and 3 show the effect of the  $^{13}\text{C}$  neutron source on the Si and Ti isotopic abundances inside the  $^{13}\text{C}$  pocket. The values of column 4 were calculated at the time when the *s*-enriched pocket has been engulfed by the growing convective pulse and diluted with both *s*-processed material from the previous pulse and material from the H-burning ashes, containing in particular Si and Ti of initial composition. The difference between the values of columns 4 and 5 expresses the effect of the  $^{22}\text{Ne}$  neutron source activated during the 15<sup>th</sup> pulse. Note how  $^{100}\text{Ru}$  and  $^{150}\text{Sm}$  production factors are up to three orders of magnitude larger than those of Si and Ti. From the results given in Table 2, it is easily recognized that neutron captures only marginally modify the initial Si and Ti isotopic compositions.  $^{28}\text{Si}$  tends to be slightly consumed (by 15 ‰, and by 20 ‰, respectively) after both neutron exposures. Actually, during the high neutron exposure from the  $^{13}\text{C}$  source  $^{29}\text{Si}$  is more efficiently consumed (by a factor 1.6) than produced, because of the very low cross section of  $^{28}\text{Si}$ . Also  $^{30}\text{Si}$  is consumed (by a factor 2.2) during this phase. In contrast, the abundances of both neutron-rich Si isotopes grow during the thermal pulse, by factors of about 1.3 and 1.4, respectively, relative to their initial values in the convective pulse. These features are mainly due to the fact that the neutron capture cross sections strongly depart from the  $1/v$  trend. Note that  $\sigma_{code}(^{28}\text{Si})$  is almost an order of magnitude greater at 23 keV than at 8 keV, which explains why in the TP phase this isotope is destroyed to a larger extent than in the  $^{13}\text{C}$  pocket. As a consequence, we observe the growth of  $^{29}\text{Si}$  during the TP.

Among the Ti isotopes,  $^{50}\text{Ti}$  is a neutron magic nucleus ( $N = 28$ ) and its neutron capture cross section is very small compared to those of the other Ti isotopes. It shows a strong departure from the  $1/v$  trend (see Table 1), being a factor of 4 greater at

23 keV than at 8 keV. As shown in Table 2,  $^{50}\text{Ti}$  accumulates during the  $^{13}\text{C}$  neutron exposure because of its very low neutron capture cross section, which makes this isotope a bottleneck of the abundance flow.  $^{49}\text{Ti}$  is produced in both phases, by a larger factor during the pulse, while  $^{48}\text{Ti}$  is consumed. Note that during the high neutron exposure by the  $^{13}\text{C}$  neutron source  $^{48}\text{Ti}$  is only marginally modified, despite its relatively large cross section. This results from abundance flow starting at  $^{40}\text{Ca}$ , an isotope of large initial abundance and of cross section  $\sigma_{\text{code}}(8 \text{ keV}) = 6.11 \text{ mbarn}$ , which is consequently consumed (by a factor  $\approx 6$ ) in this phase. The  $^{46}\text{Ti}$ ,  $^{47}\text{Ti}$  and  $^{48}\text{Ti}$  isotopes, similarly to the Si isotopes, suffer almost negligible variations.

Because of their relatively small cross sections, a behavior similar to that of Si and Ti is shown by other light elements below Fe, among them S and Ca. It should be emphasized that the final Si isotope composition mostly depends on the small neutron exposure by the  $^{22}\text{Ne}$  neutron source in the convective pulse rather than on the very large neutron exposure by the  $^{13}\text{C}$  neutron source taking place in the tiny radiative  $^{13}\text{C}$  pocket.

Table 2, column 6 shows the production factors in the envelope immediately after the TDU that follows the quenching of the 15<sup>th</sup> thermal pulse. At this stage, the star has become a C star, with C/O = 1.3, and the isotopic composition of the envelope results from the mixing of the *s*-processed and  $^{12}\text{C}$ -enriched material cumulatively carried into the envelope by previous TDU episodes.

Predictions for the Si and Ti isotopic compositions in the envelope of AGB stars of solar metallicity and initial mass of 1.5 and  $3 M_{\odot}$  during repeated TDUs in the TP phase are shown in Fig. 5. Fig. 6 reports predictions for the resulting Ti vs. Si correlation: as in Fig. 4, Ti ratios are plotted as function of the  $^{29}\text{Si}/^{28}\text{Si}$  ratio. They are all reported in the form of  $\delta$ -values for three different choices of the amount of  $^{13}\text{C}$  in the He intershell. The standard case (ST) of Gallino et al. (1998a) corresponds to an average mass fraction of  $^{13}\text{C}$  of  $6 \times 10^{-3}$  distributed over a tiny layer of a few  $10^{-4} M_{\odot}$  at the top of the He intershell, case d3 corresponds to the amount of case ST divided by 3 and case u2 is an upper limit corresponding to the amount of case ST multiplied by 2. As already mentioned in Busso et al. (1999a) (see also Busso, Gallino, & Wasserburg 1999b), a spread in the  $^{13}\text{C}$  amount in stars of different metallicities is required by spectroscopic observations of *s*-enhanced stars, and conceivably depends on the initial stellar mass or other physical characteristics (such as stellar rotation). The measurements of Zr, Mo, and Sr isotopic ratios in individual SiC grains have confirmed this spread in the  $^{13}\text{C}$  amount: all single grain compositions can be matched by low-mass AGB models of about solar metallicity if we consider different amounts of  $^{13}\text{C}$  (Gallino et al. 1998b; Nicolussi et al. 1998b). Open symbols are for envelopes with C/O > 1, the condition for SiC condensation. Note that case ST for solar metallicity best reproduces the *s*-process isotopic distribution of bulk SiC grains, which is slightly different from the solar main component (for a general discussion see Gallino et al. 1997; Busso et al. 1999b).

Not surprisingly the  $^{29}\text{Si}/^{28}\text{Si}$ ,  $^{30}\text{Si}/^{28}\text{Si}$ , and  $^{47}\text{Ti}/^{48}\text{Ti}$  ratios are only a few percent (up to 25 ‰, 40 ‰, and 14 ‰, respectively) higher than the corresponding solar ratios. The  $^{46}\text{Ti}/^{48}\text{Ti}$  and  $^{49}\text{Ti}/^{48}\text{Ti}$  ratios are up to 70 ‰ and 200 ‰ higher than the solar ratios. In agreement with the results shown in Table 2, the only ratio that is affected to a significant extent (up to 500 ‰ higher than solar) is the  $^{50}\text{Ti}/^{48}\text{Ti}$  ratio. Note that the  $^{50}\text{Ti}/^{48}\text{Ti}$  values range from +100 ‰ to +500 ‰, depending on the  $^{13}\text{C}$  amount.  $^{50}\text{Ti}$  is a magic nucleus whose abundance

is very sensitive to the high neutron exposure in the  $^{13}\text{C}$  pocket. The fact that the  $^{50}\text{Ti}/^{48}\text{Ti}$  ratio is significantly changed during the AGB phase is, in a way, consistent with the  $^{50}\text{Ti}/^{48}\text{Ti}$  ratios measured in SiC grains. Model predictions do not reproduce the spread of the measured Si and Ti compositions, nor could they ever explain the negative  $\delta$ -values measured in some grains; the calculated  $^{50}\text{Ti}/^{48}\text{Ti}$  ratio, though, reaches  $\delta$ -values that are higher than those of all the other Si and Ti  $\delta$ -values both in AGB model predictions and in single SiC grain measurements (up to 300 ‰, see Fig. 4).

We also investigated two other TP-AGB models: a case of  $M = 5 M_{\odot}$  of solar metallicity (Fig. 7) and a case of  $M = 3 M_{\odot}$  of 1/3 solar metallicity (Fig. 8). An interesting feature is common to both models: the maximum temperature at the bottom of the He convective shell is somewhat higher than in the models described above. As a consequence, the production factors for  $^{29}\text{Si}$  and  $^{30}\text{Si}$ , whose production is most sensitive to the  $^{22}\text{Ne}$  neutron source (see Table 2), at the end of the 15<sup>th</sup> pulse reach 3.2 and 5.9, respectively, for the  $M = 5 M_{\odot}$  star of solar metallicity, and 3.1 and 6.5, respectively, for the  $M = 3 M_{\odot}$  star of  $Z = Z_{\odot}/3$ .

This results in an increase of up to 80 ‰ and 200 ‰ in  $\delta^{29}\text{Si}/^{28}\text{Si}$  and  $\delta^{30}\text{Si}/^{28}\text{Si}$ , respectively, in the envelope of the  $M = 5 M_{\odot}$  model (Fig. 7), and of up to 100 ‰ and 200 ‰ in the 1/3  $Z_{\odot}$  model (Fig. 8). The largest  $^{29}\text{Si}$  and  $^{30}\text{Si}$  excesses measured in SiC are reproduced, however with a slope of about 0.5 for the mixing line, whereas the slope of the mainstream correlation line in the Si 3-isotope plot is 1.31 (Fig. 4). Note the extremely high values (up to 2000 ‰) reached by  $^{50}\text{Ti}/^{48}\text{Ti}$  in the last case (Fig. 8). They result from the fact that, in our AGB model, the neutron exposure in the  $^{13}\text{C}$  pocket is very sensitive to metallicity: it grows with decreasing metallicity (see Gallino et al. 1999).

As for all the cases above, the initial isotopic composition of the star has been assumed to be solar, including the  $Z = Z_{\odot}/3$  case. In principle, some enhancement for isotopes produced by  $\alpha$  captures (such as  $^{16}\text{O}$ ,  $^{20}\text{Ne}$ ,  $^{24}\text{Mg}$ ,  $^{28}\text{Si}$ ,  $^{40}\text{Ca}$  and  $^{48}\text{Ti}$ ) as well as complex secondary-like trends of many other nuclei should be taken into account in the initial composition of low-metallicity stars. This is a tricky point, for these variations have to be deduced from GCE models together with spectroscopic observations and are, in many cases, not well defined. An exercise of this kind, in connection with a possible explanation for the Si isotopic composition of SiC of type Z, can be found in Hoppe et al. (1997). For the AGB model of  $Z = Z_{\odot}/3$ , we made some tests by assuming a small enhancement of the initial  $^{28}\text{Si}$  and  $^{32}\text{S}$ , as well as of other  $\alpha$ -rich isotopes according to the spectroscopic evidence by Edvardsson et al. (1993), and small depletions in the initial abundance of the secondary-like isotopes  $^{29,30}\text{Si}$ . It turned out that the resulting Si isotope composition in the He intershell as a consequence of neutron captures was quite insensitive to the above variations, being dominated by the most abundant  $^{28}\text{Si}$ .

It has to be remarked here that several features of the predicted Si and Ti ratios (e.g., the slope in the Si 3-isotope plot) depend on the neutron capture cross sections which, for the Si as well as the Ti isotopes, are still quite uncertain, as shown in the last column of Table 1. New measurements are highly desirable for obtaining the best possible AGB model predictions.

#### 4. THE STELLAR SOURCES OF SI AND GALACTIC HETEROGENEITY

##### 4.1. Supernova sources

As Timmes & Clayton (1996) have pointed out, SNe of Type II are the dominant sources of Si in the Galaxy, especially in its early stages. At later Galactic times, SNe of Type Ia also contribute  $^{28}\text{Si}$ . The SNII models of WW95 show that  $^{28}\text{Si}$  is a primary isotope whereas  $^{29}\text{Si}$  and  $^{30}\text{Si}$  are predominantly secondary isotopes (see also Timmes & Clayton 1996 for details). This means that  $^{28}\text{Si}$  can be synthesized in early Type II SNe from a pure H and He composition, whereas the production of  $^{29}\text{Si}$  and  $^{30}\text{Si}$  requires the prior presence of primary isotopes such as  $^{12}\text{C}$ ,  $^{14}\text{N}$  and  $^{16}\text{O}$ . As a consequence, the  $^{29,30}\text{Si}/^{28}\text{Si}$  ratios of the ejecta of SNIIe increase with the metallicity of the stars. While  $^{28}\text{Si}$  is the product of explosive O burning, both  $^{29}\text{Si}$  and  $^{30}\text{Si}$  are synthesized in a narrow region by explosive Ne burning. Actually,  $^{29}\text{Si}$  production is restricted to the outer region of the Ne burning shell.

Fig. 9 shows the  $^{29,30}\text{Si}/^{28}\text{Si}$  ratios (plotted as  $\delta$ -values) of the averages of the yields of SNII models of different metallicities. The cases of metallicity  $Z=0.1\ Z_{\odot}$  and  $Z=Z_{\odot}$  are taken from WW95, the cases  $Z=0.5\ Z_{\odot}$  and  $Z=2\ Z_{\odot}$  are from more recent, unpublished calculations by Weaver & Woosley. To obtain the averages we took the initial mass function for massive stars into account by weighing the contributions from SNIIe of different masses according to  $M^{-2.35}$  per unit mass interval, the Salpeter initial mass function. Fig. 9 shows that in the WW95 models there exists a fairly good linear relationship between the  $^{29,30}\text{Si}/^{28}\text{Si}$  ratios of the average SN yields and the metallicity, demonstrating the secondary nature of the heavy Si isotopes. The GCE of the Si isotopes is thus believed to have progressed from small  $^{29,30}\text{Si}/^{28}\text{Si}$  ratios at early Galactic times to larger and larger ratios as the metallicity of the whole Galaxy increased and SNIIe of increasing metallicity contributed their Si to the ISM (Timmes & Clayton 1996).

This process is expected to have resulted in the Si isotopic ratios at the time and place of solar formation. However, closer inspection of Fig. 9 and especially Fig. 10, where the  $\delta$ -values of the  $^{29,30}\text{Si}/^{28}\text{Si}$  ratios of the averages of SNII yields are plotted in a Si 3-isotope plot, reveals that the SNII models by Weaver & Woosley do not exactly produce the solar Si isotopic composition. It is evident that  $^{29}\text{Si}$  in the presently available models is under-produced and the isotopic evolution expected from SNII contributions misses the solar isotopic composition (Fig. 10). This is a long-recognized problem: Type II SN models under-produce  $^{29}\text{Si}$  relative to  $^{30}\text{Si}$  as compared to the solar isotopic ratio (Timmes et al. 1995; Timmes & Clayton 1996; Thielemann, Nomoto, & Hashimoto 1996; Nomoto et al. 1997). This fact is also demonstrated by a comparison of model predictions and the Si isotopic ratios of type X SiC,  $\text{Si}_3\text{N}_4$ , and low-density graphite grains, all of which are believed to originate from Type II SNe (Nittler et al. 1995; Travaglio et al. 1999). The Si isotopic ratios of these grains have systematically higher  $^{29}\text{Si}/^{30}\text{Si}$  ratios than those predicted by SN models (Zinner et al. 1998; Travaglio et al. 1999). In order to achieve the solar ratios, Timmes & Clayton (1996) proposed multiplying the  $^{29}\text{Si}$  yields of SNII models by a factor of  $\sim 1.5$ . We will do likewise in this paper and multiply the  $^{29}\text{Si}$  yields by the same factor to obtain the best fit to the solar isotopic ratios or to the grain data.

It should be mentioned that there still exist major problems associated with the synthesis of the Si isotopes in massive stars. As Arnett & Bazan (1997) pointed out, heterogeneous mixing between different layers during the late evolutionary stages might have a major effect on the nucleosynthesis of certain elements. Bazan & Arnett (1998) used a two-dimensional hydro-

dynamic code to investigate convective O-shell burning in a  $20\ M_{\odot}$  star. They concluded that the results of these calculations differ in many ways from those of one-dimensional models and that corresponding changes in the nucleosynthesis of Si during this stage are to be expected. It remains to be seen whether full nucleosynthetic calculations in two- or three-dimensional models can shed light on the problem of relative yields of the Si isotopes. Another problem is the relative contribution of Type Ia and Type II SNe to the GCE of the heavy elements, in particular Fe. Whereas in the Timmes et al. (1995) GCE model Type II SNe were assumed to contribute 2/3 of the Fe in the solar system, Woosley et al. (1997) favored a more important role of Type Ia SNe, letting them contribute as much as half of the solar Fe. This would indicate somewhat higher contributions by Type Ia SNe to the Galactic  $^{28}\text{Si}$  relative to SNIIe. In addition to possible uncertainties in the nuclear physics and in the treatment of the various convective zones affecting the production of the three Si isotopes, problems are related to the effect of mass loss from the most massive stars and to Galactic enrichment by close binary massive stars (Woosley, Langer, & Weaver 1993, 1995), to the effect of rotation (Heger, Langer, & Woosley 1999), and to the still uncertain development of the explosion (WW95, Thielemann et al. 1996).

While in Fig. 9 only averages of SNII models of different metallicities have been plotted, it has to be realized that SN models of different masses yield very different Si isotopic ratios. In Fig. 10, in addition to averages, we also plotted the isotopic ratios of individual SNII models of different masses for the  $Z=0.1\ Z_{\odot}$  and the  $Z=Z_{\odot}$  case. The yields and Si isotopic ratios for the  $Z_{\odot}$  case are also given in Table 3. As can be seen, the isotopic ratios of different mass SNIIe span a wide range. There are variations not only in the  $^{29,30}\text{Si}/^{28}\text{Si}$  ratios but also in the  $^{29}\text{Si}/^{30}\text{Si}$  ratio. The last column in Table 3 shows the latter ratio (already readjusted by augmenting the  $^{29}\text{Si}$  yield) for SNIIe of different mass. Note that the ratio is smaller than unity for most SNIIe of lower mass but larger than unity for the two most massive models. In Fig. 11 we plotted again the average Si isotopic ratios for the  $Z_{\odot}$  case together with the averages for the SN models with masses  $M \leq 25\ M_{\odot}$  and  $30\ M_{\odot} \leq M \leq 40\ M_{\odot}$ . This time the theoretical  $^{29}\text{Si}$  yield was increased by the same factor 1.5 for Type II SNe of all masses in such a way that the weighted average ratios plot on the slope-one line or, in other words, that the average  $^{29}\text{Si}/^{30}\text{Si}$  ratio is solar. As can be seen, the low-mass average falls slightly below the slope-one line through the origin (pure  $^{28}\text{Si}$ ) and the solar isotopic composition and the high-mass average falls above this line.

While the evolution of the Si isotopes of the Galaxy as a whole and of the average of material in an annulus of a given Galactic radius undoubtedly followed the slope-one line, we expect certain variations in the Si isotopic ratios even at a given time and a given Galactic radius in relatively small regions from which low-mass stars formed. The reason is that the addition of contributions from individual SNe, which are responsible for the Si isotopic ratios of a certain region, is a stochastic process and we do not expect that material from these contributions is instantly homogenized with preexisting material. Fluctuations result from the fact that individual SN sources have yields with very different Si isotopic compositions as is clearly shown in Figs. 10 and 11. In addition to the isotopic ratios of Type II SNe, in Figs. 10 and 11 as well as in Table 3 we show also the ratios of the W7 SNIa model (Thielemann et al. 1986; updated by Nomoto et al. 1997) and the SNIa model originating from sub-Chandrasekhar (hereafter sub-Ch) white dwarfs

accreting He from a binary companion (Woosley & Weaver 1994). These SN types are believed to be the major sources of Si in the Galaxy around the time of solar system formation (Timmes & Clayton 1996; Woosley et al. 1997).

Let us now consider the effect on the Si isotopic ratios of the admixture of material from one of these SN sources to material with a given isotopic composition (Fig. 11). Three-isotope plots such as those shown in Figs. 10 and 11 have the property that the isotopic composition of a mixture between two components lies on a straight line connecting the isotopic ratios of the two components. For the sake of demonstration we arbitrarily selected as starting composition the Si isotopic composition of the sun. Admixture of different SN sources (we chose SNIa W7, SNIa sub-Ch, and, again for the sake of demonstration, the low- and high-mass averages of the  $Z_{\odot}$  Type II SN models of WW95) will shift the starting composition in the directions of the arrows in the figure (see also Figs. 8 of Timmes & Clayton 1996 for mixtures between average ISM and ejecta from individual SNe). These authors also mentioned the possibility of reproducing a larger-than-unity slope for the Si isotopic ratios of the mainstream SiC grains but did not systematically develop the local heterogeneity picture as it is done in this work). Thus admixture of material from a SNIa sub-Ch will shift the composition toward the origin (pure  $^{28}\text{Si}$ ). We note that the average of the high-mass SNII sources (with adjusted  $^{29}\text{Si}$  yield) lies above the slope-one line from the origin through the solar composition. This means that admixture of material from these sources will shift, on average, the original solar composition along a line with a slope larger than one. Likewise, because the average of the low-mass sources lies below the slope-one line, admixture from these sources will again, on average, result in a shift along a line with a slope larger than one. The same is true, even though to a lesser extent, if material from the Type Ia W7 SN model (containing essentially pure  $^{28}\text{Si}$ ) is added to the solar composition.

#### 4.2. Monte Carlo calculations

If contributions from a limited number of such sources are considered, the resulting Si isotopic compositions will fluctuate from one mix to the next because of the statistical nature of these contributions. We have developed a simplified Monte Carlo (MC) model in which we add material from a limited number of discrete SN sources in a statistical way to material with an arbitrary (but reasonable) starting isotopic composition in order to see whether the Si isotopic distribution of the mainstream SiC grains can be explained as the result of statistical fluctuations or, in other words, local heterogeneities in the regions where low-mass stars - as AGB stars the sources of mainstream grain - were born. A detailed description of our MC model can be found in the Appendix.

We have performed different calculations with different assumed starting compositions. As first test we took the average Si isotopic ratios of the mainstream SiC grains corrected for AGB contributions ( $\delta^{29}\text{Si}/^{28}\text{Si}_{\text{mean}} = 30.4\text{ }/\text{o}$  and  $\delta^{30}\text{Si}/^{28}\text{Si}_{\text{mean}} = 27\text{ }/\text{o}$  - see Appendix) as starting composition. In other words, we considered the mean composition of the mainstream grains' parent stars as a possible "standard" composition of the ISM from which these stars were born. We then randomly added  $N$  SN contributions and randomly chose the sign of each contribution (i.e., the sign of the parameter  $a$ , the constant factor by which the total mass ejected by each SN is multiplied) in order to simulate material that could have seen more or less from each kind of SN source relative to the chosen standard

ISM composition. In this way we generated 200 different mixtures, whose isotopic ratios are plotted Fig. 12a. The plot shows the case for  $N = 100$ . For  $a$ , the fraction taken from each SN source, we obtained  $a = 1.5 \times 10^{-5} M_{\odot}^{-1}$ . Note that because we computed abundances for each isotope  $i$  in the form of mass fractions  $X_i$  (see Appendix), the contributing terms  $a \times M_{\text{ejected}}$  do not have a dimension and the parameter  $a$  has the dimension of the inverse of a mass. As explained in the Appendix, because of the limited number (200) of cases, a certain range of the parameter  $N$  is expected to yield a good fit. Other similarly good matches are obtained for values of  $N$  ranging between  $\sim 50$  and  $\sim 200$ , and  $a$  accordingly from  $\sim 1.9 \times 10^{-5} M_{\odot}^{-1}$  and  $\sim 0.95 \times 10^{-5} M_{\odot}^{-1}$ . In Fig. 12a we also took the modification of the Si isotopes by nucleosynthesis in the AGB parent stars into account, adding the average isotopic shift given above to the results of the Monte Carlo calculation. As can be seen from the figure, the 200 different mixtures generated with these parameters by MC in a random fashion match the distribution of the grains surprisingly well. We note that the slope of the correlation line of the MC points is larger than unity but somewhat smaller than the slope of 1.31 of the mainstream correlation line. The slope of the MC compositions reflects the distribution of the SN sources, mostly the SNII sources of solar metallicity. As has been already pointed out above in the discussion of Fig. 11, these sources are aligned with an average slope that is greater than one.

If we choose starting compositions different from the average of the mainstream SiC grains, it turns out that for a wide range of starting Si isotopic ratios, as long as they are constrained to be compositions expected for the Galactic evolution of the Si isotopes (i.e., compositions that in Si 3-isotope plots such as those in Figs. 10 and 11 lie on the slope-one line between the origin representing pure  $^{28}\text{Si}$  and the solar isotopic composition), values for the parameters  $N$  and  $a$  can be found that let us achieve a good match with the Si isotope distribution of the mainstream SiC grains, albeit with different choices of the parameters  $N$  and  $a$  for each case. We investigated three more cases for which we chose  $a$  always to be positive. The results are shown in Figs. 12b, 12c, and 12d. In the first of these cases the starting isotopic composition is solar, in the second case Si is depleted in the heavy isotopes by  $100\text{ }/\text{o}$  ( $\delta^{29}\text{Si}/^{28}\text{Si}_{\text{init}} = -100\text{ }/\text{o}$  and  $\delta^{30}\text{Si}/^{28}\text{Si}_{\text{init}} = -100\text{ }/\text{o}$ ) and in the third by  $200\text{ }/\text{o}$ . The best-fit parameters are  $N = 70$  and  $a = 1.7 \times 10^{-5} M_{\odot}^{-1}$  for the first case,  $N = 420$  and  $a = 1.1 \times 10^{-5} M_{\odot}^{-1}$  for the second case, and  $N = 600$  and  $a = 1.5 \times 10^{-5} M_{\odot}^{-1}$  for the third case. Also in these cases, we obtain good fits for a range of  $N$  and  $a$  values.

It is clear that the addition of SN material will change the concentration of other elements as well. As the statistical nature of these additions results in a range of Si isotopic ratios, we expect it to result in a corresponding range of elemental ratios as well and these variations can be compared with astronomical observations in stars. In Fig. 13a we plotted the scatter in elemental ratios obtained by the MC calculation for the case with  $\delta^{29}\text{Si}/^{28}\text{Si}_{\text{init}} = \delta^{30}\text{Si}/^{28}\text{Si}_{\text{init}} = 0$ . In different Galactic regions elemental ratios relative to H are expected to be affected by newly infalling gas and not only by the contributions from stellar nucleosynthesis. For this reason we plotted ratios relative to Fe and normalized to the solar system abundances (i.e.,  $[\text{Elem}/\text{Fe}] = \log[(\text{Elem}/\text{Fe})/(\text{Elem}/\text{Fe})_{\odot}]$ ). The spreads in the theoretical elemental ratios are quite modest, especially if compared with ratios observed in stars. Edvardsson et al. (1993) measured elemental abundances in a large number of stars from the Galaxy

and concluded that stars from a given epoch (i.e. of a given age) and from a given Galactic radius show a considerable spread in metallicity. That this spread is not simply the result of variations in the amount of newly infalling material is shown by the fact that also elemental ratios between elements, in particular relative to Fe, show considerable variations (Fig. 13b). Edvardsson et al. (1993) pointed out that, despite observational errors (including a typical uncertainty of 1 - 2 Gyr in the age of dwarf stars), these variations are intrinsic (see also Timmes et al. 1995). A comparison of Figs. 13a and 13b shows that the spread in elemental ratios obtained from a model of statistical fluctuations in the contributions from various SN sources is smaller than the spread observed in stars. Since we do not know exactly how much of the spread in the Edvardsson et al. (1993) data is due to experimental errors, we just want to emphasize that the MC spread is not larger than that in stars. The models by Copi (1997) and van den Hoek & de Jong (1997), which make use of stochastic approaches in the study of GCE, are able to account for these elemental spreads. The mass of a well-mixed region (a sort of mixing scale) that in the Copi (1997) model yields a good fit to the spread of the abundances of  $\alpha$ -elements (such as Si) in stars is  $M \sim 10^5 M_\odot$ . If we interpret our constant parameter  $a$  as the inverse of the total mass of the region in which the SN ejecta are expected to be well mixed, we find for this region a mass of  $M = 1/a \sim 10^5 M_\odot$ , a number remarkably similar to that found by Copi (1997).

We conclude that local heterogeneities in Galactic regions that can explain the variations in Si isotopic ratios observed in the mainstream SiC grains imply variations in elemental ratios that are compatible with those observed in stars. In principle, such heterogeneities could be the cause of the mainstream isotopic variations.

#### 4.3. Discussion

It has to be emphasized that our model for explaining the Si isotopic variations in mainstream SiC grains does not pretend to fully simulate the isotopic compositions of the SiC mainstream grains. It uses theoretical yields of the Si isotopes ejected from SNe that needed adjustment to explain the composition of the solar system (see section 4.1). In addition, the model is overly simplistic and at this point should only be understood as a demonstration that local heterogeneities due to the statistical nature of SN contributions can in principle successfully reproduce these variations. In reality the situation is expected to be much more complicated:

- 1) There will be a statistical spread in the individual SN contributions;
- 2) There will be a spread in the initial composition;
- 3) There will be contributions from SNe with a range of metallicities;
- 4) There will be a range in ages of the AGB stars because of differences in their mass.

We will discuss these points in turn.

- 1) We assumed that all the SN sources that add material to a given Galactic region contribute the same amount as expressed by a single value of the parameter  $a$ . In reality different SNe will contribute different amounts and in some extreme cases one SN will completely dominate the

local mix. In our MC calculations we have also assumed different statistical distributions for the parameter  $a$  and could achieve essentially the same final results as those shown in Figs. 12.

2) We have shown that different initial Si isotopic compositions can produce distributions close to that of the mainstream grains if the parameters for the admixture of SN material (number of SN sources,  $N$ , and fraction of Si ejected by a SN,  $a$ ) are chosen appropriately. In reality we have to expect a whole range of initial compositions reflecting different times and different degrees of homogenization of matter in the Galaxy. We expect that material at a given Galactic radius is homogenized on a time scale of less than  $10^8$  yr, the period of Galactic rotation. Any complete homogenization will destroy the local heterogeneities in which we are interested. The real local isotopic compositions will represent some balance between heterogeneity and processes of homogenization. The overall result will be the GCE of the elements and the isotopes, the overall trend being modified by local fluctuations.

3) In our model we have considered only Type II SNe of solar metallicity. In reality there will be a range of metallicities. This is for two reasons. First, we expect to encounter some range in age for AGB stars as will be discussed in the next section. Second, if local regions are highly contaminated with previous SN contributions, new SNe from such regions will have higher-than-average metallicities. According to the WW95 SNII models the addition of SNIIe ejecta of a given metallicity to an ISM parcel of the same metallicity will result in higher  $^{29}\text{Si}/^{28}\text{Si}$  and  $^{30}\text{Si}/^{28}\text{Si}$  ratios than those of the starting material. This reflects the fact that  $^{29}\text{Si}$  and  $^{30}\text{Si}$  are secondary isotopes. The enrichment of the heavy Si isotopes in Type II SN ejecta over the average ISM material has first been pointed out by Clayton (1988) on the basis of an idealized GCE model. The enhancement of  $^{29}\text{Si}$  and  $^{30}\text{Si}$  in the SNII ejecta over the starting composition is clearly seen in Fig. 11 for SNIIe of solar metallicity, where the average value plots to the upper right of the solar Si isotopic composition (this includes an assumed enhanced production of  $^{29}\text{Si}$ ). However, a minimum metallicity is required for the contributing SNIIe in order to achieve the average Si isotopic ratios of the protosolar nebula or those of the mainstream grains. We conclude from Fig. 9 that a metallicity of  $Z > 0.75 Z_\odot$  is required for the average Si isotopic composition of SNII ejecta to be heavier than 150 ‰, the maximum of the mainstream grains. This, however, is a lower limit since in reality low-mass stars do not form from pure SN ejecta.

4) It has to be clear that the Si isotopic compositions of the mainstream grains reflect those of their parent stars at the time of their birth and it is these compositions that we want to explain. However, it is also clear that, depending on their mass, different stars were born at different Galactic times, even if they all produced SiC grains at the same time during their AGB phase (and even this last assumption is not strictly valid because different SiC grains could have different IS life times between their formation and the birth of the solar system). So far we have made the implicit assumption that grains came only

from stars in the  $1.5 - 3 M_{\odot}$  range when we computed the inferred Si isotopic ratios of the mainstream grains without any AGB contributions (i.e., the initial isotopic ratios of the parent stars). In the following subsection we want to explore this question in more detail.

The processes leading to heterogeneity in the Si isotopic ratios in the ISM are much more complex than the simple mixing assumed in our MC model. However, and this is the most important conclusion of our tests, it is practically certain that the ISM at a given Galactic time and at a given Galactic radius is not characterized by a unique Si isotopic composition but by a range of compositions. This distribution of Si ratios will shift toward heavier isotopic ratios during the evolution of the Galaxy. Note that presently we do not know the exact distribution of the Si isotopes at a given Galactic time nor the relationship between Galactic time and the mean of the Si isotopic ratios of the distributions. For the time being we assume that the latter is the same as that of the Timmes & Clayton (1996) model, but this point will be discussed in more detail in §4.5.

#### 4.4. The mass of the SiC parent stars

In §3 and Figs. 5 - 8 we showed that the shift in Si isotopic compositions due to neutron capture in the He shell of AGB stars depends on stellar mass and metallicity. As we demonstrated in that section, the changes in the Si isotopic composition due to the *s*-process in AGB stars depend almost entirely on the small neutron exposure from the  $^{22}\text{Ne}$  source, with the  $^{13}\text{C}$  pocket having no influence, independent of the magnitude of its strength. The effects on stellar mass and metallicity we are discussing in this section actually are the results of complete stellar evolutionary calculations of the AGB phases using the FRANEC code. At solar metallicity, from a  $5 M_{\odot}$  complete AGB evolutionary model we find a somewhat higher maximum temperature at the bottom of the He thermal pulses than in lower mass stars ( $1.5 M_{\odot}$  to  $3 M_{\odot}$ ). Because the  $\alpha$ -capture reaction rate is proportional to  $T^{21}$ , this higher temperature increases the efficiency of the neutron burst from the  $^{22}\text{Ne}$  source, correspondingly changing the predicted final Si ratios as illustrated in the figures.

The same tendency is found in stellar evolutionary calculations with the FRANEC code for AGB stars of different mass and a metallicity of  $1/3 Z_{\odot}$ , as shown in Table 4. The maximum temperature at the bottom of the thermal pulse increases slightly from pulse to pulse, starting from about  $2.65 \times 10^8$  K for the pulse when TDU occurs for the first time. The temperature during the pulse rises in a very rapid burst; subsequently the bottom temperature decreases more or less exponentially from its maximum, with a total duration time (at  $T > 2.5 \times 10^8$  K) of a few years.

Whereas for  $1.5 M_{\odot}$  and  $3 M_{\odot}$  stars of solar metallicity the maximum shifts in  $\delta^{30}\text{Si}/^{28}\text{Si}$  are only  $26 \text{ \textperthousand}$  and  $37 \text{ \textperthousand}$ , respectively, the maximum shift for a  $5 M_{\odot}$  star is  $180 \text{ \textperthousand}$ . In Figs. 14a-d we plotted the results of the MC calculations for the  $-100 \text{ \textperthousand}$  case if we add the shifts expected for AGB stars of masses  $1.5 M_{\odot}$ ,  $3 M_{\odot}$ , and  $5 M_{\odot}$  with solar metallicity and of  $3 M_{\odot}$  with  $Z = 0.006$ . The ranges of shifts were added in a random, statistical fashion in our MC test. As can be seen, only the  $1.5 M_{\odot}$  and  $3 M_{\odot}$  stars of solar metallicity give results in reasonable agreement with the grain data, while  $5 M_{\odot}$  stars as well as stars with  $Z = 0.006$  shift the Si isotopic compositions far to the right of the grain data and the solar composition. Especially for the low-metallicity case of Fig. 14d the predicted

shifts have a much wider spread. It is a remarkable result of our heterogeneity model that, without any AGB contributions, the solar composition is one of the possible compositions and at the same time the mainstream data can be reproduced if the AGB shifts are small, as for the  $1.5 M_{\odot}$  and  $3 M_{\odot}$  star models of close-to-solar metallicity. This is not true anymore if the AGB shifts are as large as those for  $5 M_{\odot}$  stars.

From the above discussion, it is reasonable, even if not proven, to assume that mostly low-mass stars (with  $M \leq 3 M_{\odot}$ ) contributed SiC to the solar system. Actually, there are many pieces of evidence that indicate that this is indeed the case:

- 1) Feast (1989) performed a study of the kinematics of peculiar red giants including S, SC, and C stars. On the basis of 427 C stars he estimated their mean mass to be  $1.6 M_{\odot}$ . Although this estimate needs to be improved, if SiC grains came from average C stars, they came from low-mass stars.
- 2) Another argument for low masses of carbon stars is based on a comparison of the observed luminosities of AGB stars in the Magellanic clouds with predicted luminosities. Theory predicts intermediate-mass stars of  $5 - 8 M_{\odot}$  to have  $M_v$  of less than  $-6.5$  but typical luminosities of S and C stars are much lower, indicating low-mass stars (Mould & Reid 1987; Frogel, Mould, & Blanco 1990; Van Loon et al. 1998).
- 3) Another argument is based on theoretical predictions about the occurrence of hot bottom burning (HBB) in intermediate-mass ( $5 - 8 M_{\odot}$ ) stars. HBB takes place when the bottom layers of the convective envelope are hot enough for some proton capture nucleosynthesis to occur. In this case, most  $^{12}\text{C}$  dredged up from the He shell during the TP-AGB phase is converted to  $^{14}\text{N}$ , preventing the star from becoming a carbon star. There are several theoretical studies that indicate that HBB occurs in stars of  $\gtrsim 5 M_{\odot}$  of solar metallicity and in stars with  $\gtrsim 4 M_{\odot}$  of lower metallicity (Boothroyd, Sackmann, & Wasserbburg 1995; Forestini & Charbonnel 1997; Lattanzio et al. 1997). For solar metallicity stars, the FRANEC code finds HBB in a  $7 M_{\odot}$  but not a  $5 M_{\odot}$  star. The situation is complicated by the finding that if HBB stops while thermal pulses and TDUs continue in a star with mass loss, the star can become C-rich (Frost et al. 1998; Lattanzio & Forestini 1999). However, this happens only in low-metallicity stars. Furthermore, if superwinds during the advanced AGB phase erode the envelope quickly, it is possible that TP cease before the star becomes C-rich. Thus, by and large it is not very likely that there are a substantial number of C-rich intermediate-mass stars that could have contributed SiC to the solar system.
- 4) We also obtain constraints on the mass and the metallicity of the parent stars from the isotopic compositions measured in presolar SiC grains when these compositions are compared with model calculations:
  - i) It has already been pointed out that the heavy elements patterns measured in presolar SiC are well reproduced by models of neutron-capture nucleosynthesis in AGB stars (Gallino et al. 1997). However, this agreement exists only for low-mass AGB stars of close-to-solar metallicity and not for

intermediate-mass stars, or of AGB stars of low metallicity. A particularly diagnostic isotopic ratio is the  $^{96}\text{Zr}/^{94}\text{Zr}$  ratio. The large  $^{96}\text{Zr}$  depletions measured in mainstream SiC grains (Nicolussi et al. 1997; Pellin et al. 1999) are well reproduced only with models of AGB stars of  $1.5 - 3 M_{\odot}$  and about solar metallicity (Gallino et al. 1998b), but higher-mass stars and stars with low metallicity are predicted to produce huge  $^{96}\text{Zr}$  excesses.

ii) Gallino et al. (1990) pointed out that the He and Ne isotopic data of presolar SiC grains are best explained in terms of nucleosynthesis in low-mass AGB stars of close-to-solar metallicity (see their Fig. 1). Another important observation is that SiC grains do not show large  $^{25}\text{Mg}$  excesses (within relatively large errors). This again indicates low-mass stars in which  $^{22}\text{Ne}$  does not burn. Indeed, the FRANEC code yields  $^{25}\text{Mg}$  excesses of up to  $\sim 200\text{ \%}$  in the envelope of  $1.5$  and  $3 M_{\odot}$  AGB stars of solar metallicity, whereas predicted excesses are an order of magnitude larger in the  $5 M_{\odot}$  model of  $Z=0.02$  and in the  $3 M_{\odot}$  model of  $Z=0.006$ .

iii) The situation is similar with regard to the  $^{12}\text{C}/^{13}\text{C}$  ratios, where the observed range is best reproduced by low-mass AGB models of close-to-solar metallicity (Gallino et al. 1990; Bazan 1991). New results from the FRANEC code confirm these earlier conclusions: the best agreement is obtained for  $1.5 M_{\odot}$  ( $^{12}\text{C}/^{13}\text{C} = 40 - 60$ ) and  $3 M_{\odot}$  ( $^{12}\text{C}/^{13}\text{C} = 90 - 100$ ) AGB stars of solar metallicity, the  $5 M_{\odot}$  model of solar metallicity and the  $3 M_{\odot}$  model of low metallicity ( $Z=0.006$ ) yield much higher ratios ( $^{12}\text{C}/^{13}\text{C} = 90 - 120$  and  $100 - 700$ , respectively). In low-mass star models with  $M \lesssim 2.5 M_{\odot}$ , the presence of cold bottom processing (CBP) (Charbonnel 1995; Wasserburg et al. 1995; Boothroyd & Sackmann 1999) lowers the initial  $^{12}\text{C}/^{13}\text{C}$  ratio at the beginning of the TP-AGB phase.

iv) Cold bottom processing is also important for the  $^{14}\text{N}/^{15}\text{N}$  ratio. The high ratios observed in many individual mainstream SiC grains (Fig. 1) can only be explained by CBP (Huss et al. 1997) operating in low-mass stars.

5) A lower limit on the masses of carbon stars can be obtained from models with TDU. Existing models predict TDU only for stars with  $M \gtrsim 1.5 M_{\odot}$  (Lattanzio 1989; Straniero et al. 1997; Gallino et al. 1998a; Busso et al. 1999b). In the FRANEC code the limit depends on the value of Reimer's parameter  $\eta$  used. For a star of  $M = 1.5 M_{\odot}$  of solar metallicity the limit is  $\eta=0.3$  for TDU to occur and for producing  $\text{C}/\text{O} > 1$  in the envelope during the advanced stages of the AGB phase. The fact that there is a minimum mass below which TDU does not occur is of great importance, since because of it SiC grains cannot originate from long-lived stars of low mass and low metallicity. It is worth noting that increasing the metallicity above solar works against an AGB star to become C-rich. In our calculations the star remains O-rich at  $Z = 2 \times Z_{\odot}$  for  $M = 1.5 M_{\odot}$ , and already at  $Z = 1.25 \times Z_{\odot}$  for  $M = 3 M_{\odot}$ .

From all these considerations it appears that most presolar SiC grains come from AGB stars of  $1.5 - 3 M_{\odot}$  and close-to-solar metallicity. Of course, it is not said that the mainstream SiC grains have to come from typical carbon stars. It is possible that these very large grains preferentially originated from stars with very dense winds and thus from stars having masses at the upper end of the above range. However, stars with masses much larger than  $3 M_{\odot}$  can definitely be excluded.

#### 4.5. Star lifetimes, grain lifetimes and Galactic chemical evolution

Let us now return to the question of lifetimes of the possible source stars for SiC grains. Whereas the calculated lifetime of a  $5 M_{\odot}$  star of solar metallicity is  $1.1 \times 10^8$  yr (Schaller et al. 1992), those of the  $3 M_{\odot}$  and  $1.5 M_{\odot}$  stars are  $4.4 \times 10^8$  and  $2.9 \times 10^9$  yr, respectively. Especially the latter lifetime would result in a non-negligible difference in the Si isotopic ratios due to the overall temporal evolution of the Si isotopes in the Galaxy. According to the model of Timmes & Clayton (1996) a time difference of  $2.9 \times 10^9$  yr corresponds to a difference of  $125\text{ \%}$  in the  $^{29}\text{Si}/^{28}\text{Si}$  and  $^{30}\text{Si}/^{28}\text{Si}$  ratios, which is almost the whole range covered by the mainstream grains. This means that a star that was born  $2.9 \times 10^9$  yr before the sun should have  $^{29}\text{Si}/^{28}\text{Si}$  and  $^{30}\text{Si}/^{28}\text{Si}$  ratios that are, on average,  $125\text{ \%}$  smaller than the solar ratios. It also means that if stars of different mass and therefore different lifetimes contributed SiC grains to the solar system, these grains are expected to have different Si isotopic compositions. There are several factors that play a role here. One is the initial mass function for stars. There are more stars of lower mass and we have already pointed out that the estimated mean mass of carbon stars is  $\sim 1.6 M_{\odot}$  (Feast 1989). On the other hand, the fact that SiC grains are relatively large suggests that more massive AGB stars with very dense winds, meaning high mass loss at low speed, were selected as the SiC grains' parent stars.

Let us consider two extreme cases. First we consider the case that all or most of the mainstream SiC grains came from AGB stars of approximately the same mass and therefore also the same time of formation. In this case time differences do not play a role and the distribution of the Si isotopic ratios of the mainstream grains can in principle be explained as having an origin in local isotopic heterogeneities due to the statistical nature of SN contributions to the ISM. This is schematically shown in Fig. 15a where the whole range of Si isotopic compositions exhibited by the SiC mainstream grains is interpreted as the spread in Si isotopes that existed at the time of formation of the grains' parent stars. These parent stars have to have approximately the same mass but at this point it is not said whether it is low ( $1.5 M_{\odot}$ ) or high ( $3 M_{\odot}$ ).

The second case to be considered is one in which AGB stars of a *considerable* mass range contributed the mainstream grains to the solar system. In this case the range in Si isotopic shifts due to the formation time difference between stars of  $1.5 M_{\odot}$  and of  $3 M_{\odot}$  is of the same order of magnitude as the spread of the mainstream grains. Variations in the Si isotopic ratios of individual grains are expected to arise from the age differences of their parent stars (which in turn vary because of GCE) and local heterogeneities of the Si isotopes play a complementary role. This situation is schematically depicted in Fig. 15b, where the spread of the mainstream grains' Si isotopic ratios is interpreted as a superposition of local heterogeneity distributions representative of different Galactic times.

Another factor that plays a role here is the lifetime of the SiC grains in the ISM. This lifetime has to be added to the lifetime of the AGB parent stars in terms of time differences between the birth of these stars and the formation of the solar system and the implication of these time differences for the Si isotopic ratios. Unfortunately, at present we do not have any good direct measure of grain lifetimes. Attempts have been made to determine IS grain lifetimes from the measurement of cosmogenic  $^{21}\text{Ne}$  produced in the grains from the spallation of Si by Galactic cosmic rays (Tang & Anders 1988b; Lewis et al. 1994). Estimates obtained in this way range up to  $1.3 \times 10^8$  yr. However, besides poor knowledge of the flux of Galactic cosmic rays, there are many other uncertainties associated with this approach. Single grain measurements showed that only  $\sim 5\%$  of all SiC grains are rich in  $^{22}\text{Ne}$  (Nichols et al. 1991, 1992, 1993). If one assumes that outgassing is the reason that the other grains lack measurable amounts of  $^{22}\text{Ne}$  and that the same process removed cosmogenic  $^{21}\text{Ne}$  from these grains, one arrives at much higher estimates for IS grain lifetimes. However, it is unclear that outgassing is indeed the cause for the large variations of  $^{22}\text{Ne}$  among single SiC grains. Another problem is the determination of spallation recoil loss from the grains. From experimental measurements of spallation recoil Ott & Begemann (1997, 1999) concluded that a determination of presolar exposure ages from cosmogenic  $^{21}\text{Ne}$  is not feasible. These authors propose the use of spallation Xe as more promising but before this is done we do not have any reliable IS lifetimes for presolar grains. An alternative way is to use model ages derived from theoretical destruction rates of IS grains by SN shocks and collisions (see, e.g., Whittet 1992; Jones et al. 1997). Estimates range up to  $\sim 10^9$  yr but there are also large uncertainties in this approach.

#### 4.6. SiC grains and the Si isotopic composition of the sun

So far we have discussed differences in the formation time of AGB stars of different masses that possibly contributed SiC grains to the solar system. We have not discussed yet the relationship between the formation time of the grains' parent stars relative to that of the solar system and implications for their relative Si isotopic compositions. In the Timmes & Clayton (1996) model the fact that most mainstream grains have isotopically heavier compositions than the solar system (implying that they are younger) but must have formed before the sun presents a fundamental problem. Our heterogeneity model alleviates this fundamental problem, because in principle it can explain the spread in the Si isotopic compositions of the mainstream grains as inhomogeneities of the Si isotopes in the ISM at a given time (see Fig. 15a). However, the grains' parent stars must have formed before the solar system and we must discuss the effect of this time difference on their Si isotopic compositions.

For the sake of discussion we again consider two extreme cases. First we consider the case that most mainstream SiC grains came from AGB stars of  $3 M_{\odot}$ . The evolution time of such stars is  $4.4 \times 10^8$  yr. According to Timmes et al. (1995) and Timmes & Clayton (1996), such a time difference corresponds to a shift of  $19\text{‰}$  of the Si isotopic ratios. If we assume that the spread in Si isotopic ratios at the time of the birth of the parent stars coincides with that of the mainstream grains, the Si isotopic distribution at the time of solar system formation  $4.4 \times 10^8$  yr later is isotopically heavier by  $19\text{‰}$  (Fig. 16a). This shift is relatively small compared to the range of the mainstream grains. The Si isotopic composition of the sun, while falling at the outer edge of this distribution, lies still within the

range of compositions expected to be present at the time of solar system formation. The fact that the sun has a composition that differs from those of most of the grains, is not a fundamental problem in this case. It simply means that the sun, as many other SiC parent stars, has an unusual composition but one that is not incompatible with expectations.

Let us next consider the other extreme, that all grains come from stars of  $1.5 M_{\odot}$ . The evolution time of these stars is  $2.9 \times 10^9$  yr. According to Timmes & Clayton (1996) this time difference corresponds to a shift of the Si isotopic ratios by  $125\text{‰}$ . This means that the distributions of the Si isotopes at the time of star formation and at the time of solar system formation  $2.9 \times 10^9$  yr later are shifted by this amount relative to one another. This is shown in Fig. 16b where, again, we assume that the Si isotopic distribution of the stars coincides with that of the mainstream grains. This time, the inferred distribution  $2.9 \times 10^9$  yr later is shifted so much that it seems quite impossible that the solar system composition observed today can be explained as being part of this distribution. In other words, in the extreme case in which only stars of  $M = 1.5 M_{\odot}$  contributed SiC grains, we are faced with the same fundamental problem as the Timmes & Clayton (1996) model, namely that the actual solar system composition is much too light compared to the distribution predicted for the time of solar system formation if the mainstream grains came from old stars.

Clayton (1997) has addressed this problem and has proposed a solution in terms of a systematic difference in the Galactic radius at which the parent stars of the mainstream grains on the one hand and the sun on the other hand formed. The parent stars are assumed to have formed at smaller Galactic radii where the metallicity and  $^{29}\text{Si}/^{28}\text{Si}$  and  $^{30}\text{Si}/^{28}\text{Si}$  ratios are believed to be higher. His model involves the diffusion of stars from smaller to larger Galactic radii due to scattering on IS clouds, following the stellar orbital diffusion model by Wielen, Fuchs, & Detlbarn (1996). Such a model had been proposed in order to explain the spread in elemental abundances observed in stars. However, a more detailed quantitative treatment by Nittler & Alexander (1999b) shows that with reasonable assumptions a diffusion model cannot account for the isotopically heavy Si compositions of the grains relative to the sun. Furthermore, van den Hoek & de Jong (1997) pointed out that stellar orbital diffusion cannot sufficiently explain the elemental abundance variations. While we do not want to discard the orbital diffusion model, we hope that the heterogeneity explanation will give a more definitive answer to this important question. This would require a model that, by computing the Galactic evolution of the Si isotopes by taking into account incomplete mixing of different stellar yields, overcomes the problems discussed in §4.3 and all those connected to the overly simplistic nature of our approach.

It should be noted that in our estimates of the Si isotopic shifts associated with time differences we have used the Si isotopic evolutions vs. time relationship given by Timmes et al. (1995) and Timmes & Clayton (1996). This relationship crucially depends on the relative proportion in which Type Ia and Type II SNe contribute to the enrichment of the ISM in Si isotopes. Timmes et al. (1995) attributed a dominant role to Type II SNe by assuming that at the time of solar system formation they contributed 2/3 of the Fe. Woosley et al. (1997), on the other hand estimated that this fraction would be 1/2. This would mean that the  $^{28}\text{Si}$  contribution from Type Ia SNe is higher and therefore the Si isotopes evolve more slowly toward heavier compositions. This in turn would mean that a Si isotopic shift

corresponding to a given time difference (Fig. 16) is smaller than what we assumed.

In conclusion, there are still large uncertainties as to the masses of the parent AGB of the grains, the ISM life times of the grains, and the time dependence of the evolution of the Si isotopes in the Galaxy. All of these uncertainties have to be clarified before we can hope to solve the problem of the difference of the Si isotopic compositions of the mainstream SiC grains and that of the solar system.

### 5. CONCLUSIONS

Mainstream SiC grains are the major group of presolar SiC grains found in meteorites. Although there is overwhelming evidence that mainstream grains have an origin in the expanding atmospheres of AGB stars, their Si isotopic ratios show a distribution (Fig. 3) that cannot be explained by nucleosynthesis in AGB stars. The theoretically predicted Si isotopic shifts in the envelope of AGB stars are either much smaller than the range observed in the mainstream grains (for AGB models of  $M=1.5$  and  $3 M_{\odot}$  and solar metallicity) or (for AGB models of  $M=5 M_{\odot}$  and solar metallicity and  $M=3 M_{\odot}$  and  $Z=0.006$ ) show a slope of  $\sim 0.5$  correlation between the  $\delta^{29}\text{Si}/^{28}\text{Si}$  and  $\delta^{30}\text{Si}/^{28}\text{Si}$  values instead of the slope 1.31 correlation line exhibited by the grains.

The distribution of the Si isotopic ratios of the mainstream grains has previously been interpreted to be the result of GCE of the Si isotopes. In this interpretation the grains' parent stars are expected to have a range of different Si isotopic ratios if they were born at different times. In this paper we proposed an alternative explanation for the Si isotope distribution by invoking isotopic heterogeneities due to the statistical nature of the contributions of a limited number of SN sources to the IS material from which the grains' parent stars formed. The Si isotopic ratios of the ejecta of possible SN sources, classical Type Ia SNe, Type Ia SNe from sub-Ch white dwarfs, and Type II SNe of different masses, span a wide range. We developed a simple Monte Carlo model in which contributions from these SN sources were admixed in a random way to material with a given Si isotopic composition. As long as this composition lies on the theoretically expected GCE line going through the solar Si isotopic composition, we could show that, with the right choice of parameters, the distribution of the Si isotopic ratios in the mainstream grains can be successfully reproduced for a wide range of starting compositions. The parameters to be adjusted are the total number of SN sources selected and the fraction of the material ejected from each SN that is admixed to the starting material. In addition, an adjustment of the SN yield of  $^{29}\text{Si}$  by a factor of 1.5 is necessary to achieve the Si isotopic ratios of the solar system. Astronomical observations of variations of elemental ratios in stars are compatible with the predictions from our MC model.

These results demonstrate that, in principle, the mainstream distribution can be explained as the result of local fluctuation in the ISM due to the admixture of material from a limited number of SN sources to the preexisting IS matter. If the AGB stars that contributed SiC grains to the protosolar nebula were born within a short period of time (by having a narrow range of masses and the grains having short IS lifetimes), such fluctuations must have been the dominant cause of the mainstream distribution. If, however, the AGB parent stars had a large range of masses and therefore a large range of lifetimes and/or the grains themselves experienced a large range of residence times in the ISM, the parent stars must have been born at different

Galactic eras and their initial Si isotopic ratios must show considerable variations because of the varying average composition of the ISM due to the GCE of the Si isotopes. In this case we still expect that local fluctuations will be superimposed on these average compositions. To simulate these complex processes it will be necessary to apply to the Si isotopes a Galactic evolution model that is able to take both components properly into account. However, a successful model would require knowledge of the mass distribution of AGB stars that contributed SiC grains (at least in the size range of the single grains whose data are plotted in Fig. 3) and the distribution of the IS lifetimes of these grains. Both pieces of information are presently unknown and we can only hope that further progress in the study of the grains and their origin will get us closer to an answer.

We are grateful to Peter Hoppe for providing isotopic data on the Murchison KJE size fraction, to Gary Huss for providing his Orgueil data, and to Stan Woosley for providing unpublished results of the Si yields from his and Weaver's  $Z=0.5 Z_{\odot}$  and  $Z=2 Z_{\odot}$  supernova models. We are deeply indebted to Oscar Straniero, Maurizio Busso, Alessandro Chieffi and Marco Limongi for all their scientific input and thank Don Clayton for ideas and discussions. The detailed and thoughtful review by Don Clayton substantially contributed to the final version of this paper. ML gratefully acknowledges the invaluable help of John Lattanzio. EZ deeply appreciates the hospitality extended to him by Roberto Gallino during a visit to the Dipartimento di Fisica Generale of the University of Torino and the support for this visit provided by the Gruppo Nazionale di Astronomia del CNR. SA acknowledges the support for a visit to the same Department provided by the University of Torino. This work was supported by an Overseas Postgraduate Research Scheme award (ML), NASA grant NAG5-8336 (SA and EZ) and by MURST Cofin98 Progetto Evoluzione Stellare (RG).

## APPENDIX

**Appendix: Monte Carlo calculations**

The problem at hand is to calculate the Si isotopic composition of material that is obtained by mixing contributions from a *limited* number of SN sources of different types to material with a given isotopic composition and to determine whether the isotopic compositions observed in mainstream SiC grains can be reproduced in this way. If the SN contributions, whose individual Si isotopic compositions vary from one SN to the next, are admixed to the starting material in a random way, each of the resulting final mixtures will have a different isotopic composition because of the stochastic nature of this process; we will obtain a distribution of compositions. It is quite natural to apply Monte Carlo (MC) methods to generate a sample of such mixtures whose isotopic distribution can be compared with the isotopic distribution of the SiC grains.

In the MC calculations we considered as starting material one solar mass with solar elemental abundances (Anders & Grevesse 1989). One  $M_{\odot}$  is a convenient mass unit since it is of the same order of magnitude as the masses of the AGB stars that contributed SiC grains to the solar system. We performed several series of MC calculations with different initial Si isotopic ratios in each case. For each such series we started with a fixed initial Si isotopic composition. To this starting material we added contributions from  $N$  different SN sources that were selected at random from a list of candidates. As SN sources we considered Type II SNe of solar metallicity, Type Ia SNe of the W7 model and the sub-Chandrasekhar model. We assumed that on average Type II SNe represented 80%, Type Ia SNe of the W7 model 12% and Type Ia SNe of the sub-Chandrasekhar model 8% of the total number of SN sources contributing Si to the mix. These relative frequencies are those recommended by Cappellaro et al. (1997). This means that if we added contributions from  $N = 100$  SNe, *on average*, 80 of these would be of Type II, 12 of Type Ia and 8 sub-Chandrasekhar SNe. However, because of the statistical nature of this mix the exact numbers would vary from one mixture to the next.

Among the Type II SN models we selected SNe of different masses which were weighted according to a Salpeter initial mass function  $f(M)dM = M^{-2.35}dM$ . We chose a mass range of 10.5 to  $42.5 M_{\odot}$ , which is the mass range covered by the Type II SN models of solar metallicity of WW95 (Table 3). Within this mass range, a mass was chosen according to the probability of the initial mass function and the SN model of WW95 was selected whose mass was closest to the chosen mass. Thus for masses between 10.5 and 11.5 we took the  $M = 11 M_{\odot}$  model from WW95, for masses between 11.5 and 12.5 the  $M = 12 M_{\odot}$  model and so on. The final mixture thus contained contributions from both kinds of Type Ia SNe and from Type II SNe of different masses but, as already mentioned, each mix contained a different combination of these sources.

For each SN, the total ejected mass of each of the three Si isotopes was multiplied by a constant factor  $a$  and then added to the starting composition. The final amount of a given isotope  $i$  is given as the mass fraction  $X^i = X_{\text{initial}}^i + \sum_1^N a \times M_{\text{ejected}}^i (SN)$ . Thus  $N \times a$  is a measure of the total amount of material added to the starting material. Since we would like the Si isotopic composition of the mix to match the compositions of the SiC mainstream grains, we first computed the mean value and standard deviation of the  $\delta^{29}\text{Si}/^{28}\text{Si}$  and  $\delta^{30}\text{Si}/^{28}\text{Si}$  values of the mainstream grains. If we restrict ourselves to the high-quality data plotted in Fig. 3 we obtain:

$$\begin{aligned}\delta^{29}\text{Si}/^{28}\text{Si}_{\text{mean}} &= 50.4 \text{ }/\text{o}; \delta^{29}\text{Si}/^{28}\text{Si}_{\text{std.dev.}} = 42.7 \text{ }/\text{o} \\ \delta^{30}\text{Si}/^{28}\text{Si}_{\text{mean}} &= 52.0 \text{ }/\text{o}; \delta^{30}\text{Si}/^{28}\text{Si}_{\text{std.dev.}} = 30.6 \text{ }/\text{o}\end{aligned}$$

Since the grain data contain also the nucleosynthetic contributions of the AGB parent stars, we subtracted  $\delta^{29}\text{Si}/^{28}\text{Si}_{\text{AGB}} = 20 \text{ }/\text{o}$  and  $\delta^{29}\text{Si}/^{28}\text{Si}_{\text{AGB}} = 25 \text{ }/\text{o}$ , the average of the shifts predicted for 1.5 and  $3 M_{\odot}$  AGB stars (Fig. 5). This gives  $\delta^{29}\text{Si}/^{28}\text{Si}_{\text{mean}} = 30.4 \text{ }/\text{o}$  and  $\delta^{30}\text{Si}/^{28}\text{Si}_{\text{mean}} = 27 \text{ }/\text{o}$  for the mean compositions of the parent stars before their Si isotopes were affected by neutron capture during the AGB phase.

The next question is how these grain averages can be obtained by our mixing procedure. The isotopic composition of the mix is expected to depend on the relative proportion of the amount of starting material to the amount of SN contributions. Note that in this discussion we understand under mix the exact mix between the starting composition and the weighted average of the SN contributions. This mix has a unique composition and does not suffer from the statistical fluctuations caused by a stochastic admixture of individual SN contributions. Alternatively, it can be considered to be the average over a large number of statistical mixtures. If the SN contributions are small, the final Si isotopic ratios will be very similar to those of the starting material. If the SN contributions dominate, the final ratios will approach those of the weighted average of all different SN sources. On a Si 3-isotope plot the Si isotopic composition will move along a straight line from that of the starting material to that of the SN average as the ratio of SN to starting material is increased from zero to infinity (Fig. 17). Note that in Fig. 17 the SiC mainstream grain average has been corrected for the *s*-process contributions of the AGB stars.

For some value of this mixing ratio (or, in other words, for some value of  $N \times a$ ) the isotopic composition of the mix will match the average of the grain data. However, this can only be the case if in a 3-isotope plot the starting composition, the average grain composition, and the average SN composition lie on a straight line. This condition is not satisfied if we choose as a starting composition one in agreement with the expected Galactic evolution of the Si isotopes, i.e. a composition on a straight line connecting the origin with the solar isotopic composition (see Fig. 11). The reason is that the average isotopic composition of all SN sources lies far below this line (see Fig. 17). This has been discussed in detail in §4.1 and, following Timmes & Clayton (1996), we argued for an adjustment of the  $^{29}\text{Si}$  production rate by a factor  $f = 1.5$  so that the main Galactic evolution of the Si isotopes goes through the solar composition. Although the average Si isotopic ratios of the mainstream grains corrected for AGB contributions ( $\delta^{29}\text{Si}/^{28}\text{Si}_{\text{mean}} = 30.4 \text{ }/\text{o}$  and  $\delta^{30}\text{Si}/^{28}\text{Si}_{\text{mean}} = 27 \text{ }/\text{o}$ ) slightly deviate from the Galactic evolution line through the solar composition (as defined by  $\delta^{29}\text{Si}/^{28}\text{Si} = \delta^{30}\text{Si}/^{28}\text{Si}$ ), this difference is negligible and the factor  $f = 1.5$  yields a satisfactory alignment of starting composition, grain composition and SN average for all selected starting compositions (one of them is shown in Fig. 17).

With this adjustment factor we can next determine the value of  $N \times a$  (i.e. the mixing ratio between starting material and SN contributions) for which the mix matches the average of the SiC grains. For the example in Fig. 17 we obtain  $N \times a = 0.0049$ . We will obtain an exact value for  $N \times a$  only if we use the weighted average of the SN contributions or in the limit of very large values for  $N$ . For a limited number of SN sources, the Si isotopic composition of the mix will vary from one mixture to the next and the spread in the isotopic ratios is expected to vary with  $1/\sqrt{N}$ . We thus can determine the number of SN sources whose admixture will result in a spread of Si isotopic ratios that is commensurate with the spread of the grain data. For this purpose we generated a total number of 200 mixtures. This is an arbitrary number but is comparable to the number of data points for the SiC mainstream grains (Fig. 3). For these 200 cases we calculated the standard deviation from the mean of the Si isotopic ratios and determined the number  $N$  of SN sources for which these standard deviations match those of the SiC mainstream data. Strictly speaking, we would obtain an exact solution for the best fit only for an infinite number of cases. Because of the statistical fluctuations associated with a finite number of cases, one set of 200 cases will yield a different best-fit value for  $N$  than another set. In other words, for a limited number of cases we obtain a certain range for the parameter  $N$  (and consequently of  $a$ ) that yields a good fit. In summary, the requirement that the distribution of Si isotopic compositions generated by the MC mixing model matches that of the SiC mainstream data allows us to determine the parameters  $N$  and  $a$ , the number of SN sources that contribute to the final mixture and the fraction of material from each. As can be clearly seen from Fig. 17, the average Si isotopic composition of SNe of solar metallicity, adjusted for an increased  $^{29}\text{Si}$  yield, is heavier than that of the solar system and of the SiC mainstream grains and the addition of SN material will, in general, shift the composition of the mixture toward larger  $^{29}\text{Si}/^{28}\text{Si}$  and  $^{30}\text{Si}/^{28}\text{Si}$  ratios. As can be seen from Fig. 10 and Table 3, it is mostly the contributions of the Type II SNe of 30, 35 and  $40 M_{\odot}$  that contribute to this isotopically heavy composition. However, because of the form of the initial mass function, the frequencies of these high-mass SNe are low. The probability for a  $35 M_{\odot}$  SN to be among the mix considered for our MC calculation is only 3.6% and that for a  $40 M_{\odot}$  SN is 2.6%. If the total number of sources  $N$  is not large, as in the case shown in Fig. 12b, for which  $N = 70$ , it is possible that in a few cases the SN contributions can actually be isotopically light so that the resulting mixture plots to the lower left of the starting composition (which is solar in the case of Fig. 12b). This is not the case anymore if  $N$  is larger such as for the examples shown in Figs. 12c and 12d, where all the mixtures are isotopically heavier than the starting compositions,  $\delta^{29}\text{Si}/^{28}\text{Si} = \delta^{30}\text{Si}/^{28}\text{Si} = -100$  and  $-200 \text{ ‰}$ , respectively.

## REFERENCES

Alexander, C. M. O. D. 1993, *Geochim. Cosmochim. Acta*, 57, 2869  
 Alexander, C. M. O. D., & Nittler, L. R. 1999, *ApJ*, 519, 222  
 Amari, S., Anders, E., Virág, A., & Zinner, E. 1990, *Nature*, 345, 238  
 Amari, S., Hoppe, P., Zinner, E., & Lewis, R. S. 1995b, *Meteoritics*, 30, 679  
 Amari, S., Lewis, R. S., & Anders, E. 1994, *Geochim. Cosmochim. Acta*, 58, 459  
 Amari, S., Lewis, R. S., & Anders, E. 1995a, *Geochim. Cosmochim. Acta*, 59, 1411  
 Amari, S., Nittler, L. R., Zinner, E., & Lewis, R. S. 1996, *Meteoritics & Planet. Sci.*, 31, A6  
 Amari, S., Nittler, L. R., Zinner, E., & Lewis, R. S. 1997a, *Lunar Planet. Sci.*, 28, 33  
 Amari, S., Nittler, L. R., Zinner, E., & Lewis, R. S. 1997b, *Meteoritics & Planet. Sci.*, 32, A6  
 Amari, S., Zinner, E., & Lewis, R. S. 1999, *ApJ*, 517, L59  
 Anders, E., & Grevesse, N. 1989, *Geochim. Cosmochim. Acta*, 53, 197  
 Anders, E., & Zinner, E. 1993, *Meteoritics*, 28, 490  
 Arnett, D., & Bazan, G. 1997, in *Astrophysical Implications of the Laboratory Study of Presolar Materials*, ed. T. J. Bernatowicz & E. Zinner (New York: AIP), 307  
 Bao, Z. Y., & Käppeler, F. 1987, *Atom. Data Nucl. Data Tables*, 36, 411  
 Bazan, G. 1991, Ph.D. thesis, University of Illinois, Urbana-Champaign  
 Bazan, G., & Arnett, D. 1998, *ApJ*, 496, 316  
 Becker, S. A., & Iben, I. Jr. 1979, *ApJ*, 232, 831  
 Beer, H., Voss, F., & Winters R. R. 1992, *ApJS*, 80, 403  
 Bernatowicz, T. J., Amari, S., & Lewis, R. S. 1992, *Lunar Planet. Sci.*, 23, 91  
 Bernatowicz, T. J., Amari, S., Zinner, E., & Lewis, R. S. 1991, *ApJ*, 373, L73  
 Bernatowicz, T. J., Cowis, R., Gibbons, P. C., Lodders, K., Fegley, B., Jr., Amari, S., & Lewis, R. S. 1996, *ApJ*, 472, 760  
 Bernatowicz, T., Fraundorf, G., Tang, M., Anders, E., Wopenka, B., Zinner, E., & Fraundorf, P. 1987, *Nature*, 330, 728  
 Bernatowicz, T. J., & Zinner, E., 1997, in *Astrophysical Implications of the Laboratory Study of Presolar Materials*, ed. T. J. Bernatowicz & E. Zinner (New York: AIP), 750  
 Boothroyd, A. I., & Sackmann, I.-J. 1999, *ApJ*, 510, 232  
 Boothroyd, A. I., Sackmann, I.-J., & Wasserburg, G. J. 1995, *ApJ*, 442, L21  
 Brown, L. E., & Clayton, D. D. 1992a, *ApJ*, 392, L79  
 Brown, L. E., & Clayton, D. D. 1992b, *Science*, 258, 970  
 Brown, L. E., & Clayton, D. D. 1993, in *Nuclei in the Cosmos*, ed. F. Käppeler & K. Wissak (Bristol and Philadelphia: Institute of Physics), 525  
 Busso, M., Gallino, R., & Wasserburg, G. J. 1999b, *Ann. Rev. A&A*, in press  
 Busso, M., Travaglio, C., Gallino, R., Lugaro, M., & Arlandini, C. 1999a, in *Nuclei in the Cosmos V*, ed. N. Prantzos & S. Harissopoulos, (Paris: Editions Frontières), 227  
 Cappellaro, E., Turatto, M., Tsvetkov, D. Y., Bartunov, O. S., Pollas, C., Evans, R., & Hamuy, M. 1997, *A&A*, 322, 431  
 Charbonnel, C. 1995, *ApJ*, 453, L41  
 Chin, Y.-N., Henkel, C., Langer, N., & Mauersberg, R. 1999, *ApJ*, 512, L143  
 Choi, B.-G., Huss, G. R., Wasserburg, G. J., & Gallino, R. 1998, *Science*, 282, 1284  
 Clayton, D. D. 1988, *ApJ*, 334, 191  
 Clayton, D. D. 1997, *ApJ*, 484, L67  
 Clayton, D. D., Liu, W., & Dalgarno, A. 1999, *Science*, 283, 1290  
 Clayton, D. D., Obradovic, M., Guha, S., & Brown, L. E. 1991, *Lunar Planet. Sci.*, 22, 221  
 Clayton, D. D., & Timmes, F. X. 1997a, *ApJ*, 483, 220  
 Clayton, D. D., & Timmes, F. X. 1997b, in *Astrophysical Implications of the Laboratory Study of Presolar Materials*, ed. T. J. Bernatowicz & E. Zinner (New York: AIP), 237  
 Clayton, D. D., & Ward, R. A. 1978, *ApJ*, 224, 1000  
 Clayton, R. N., Hinton, R. W., & Davis, A. M. 1988, *Phil. Trans. R. Soc. Lond. A*, 325, 483  
 Cohen, M. 1984, *MNRAS*, 206, 137  
 Copi, G. J. 1997, *ApJ*, 487, 704  
 Davis, A. M., Pellin, M. J., Lewis, R. S., Amari, S., & Clayton, R. N. 1999, *Lunar Planet. Sci.*, 30, Abstract 1976  
 Dominy, J. F., & Wallerstein, G. 1987, *ApJ*, 317, 810  
 Edvardsson, B., Anderson, J., Gustaffson, B., Lambert, D. L., Nissen, P. E., & Tomkin, J. 1993, *A&A*, 275, 101  
 El Eid, M. 1994, *A&A*, 285, 915  
 Feast, M. W. 1989, in *Evolution of Peculiar Red Giant Stars*, ed. H. R. Johnson & B. Zuckerman (Cambridge: Cambridge University Press), 26  
 Forestini, M., & Charbonnel, C. 1997, *A&AS*, 123, 241  
 Frogel, J. A., Mould, J., & Blanco, V. M. 1990, *ApJ*, 96, 122  
 Frost, C. A., Cannon, R. C., Lattanzio, J. C., Wood, P. R., & Forestini, M. 1998, *A&A*, 332, L17  
 Gallino, R., Arlandini, C., Busso, M., Lugaro, M., Travaglio, C., Straniero, O., Chieffi, A., & Limongi, M. 1998a, *ApJ*, 497, 388  
 Gallino, R., Busso, M., & Lugaro, M. 1997, in *Astrophysical Implications of the Laboratory Study of Presolar Materials*, ed. T. J. Bernatowicz & E. Zinner (New York: AIP), 115  
 Gallino, R., Busso, M., Lugaro, M., Travaglio, C., Arlandini, C., & Vaglio, P. 1999, in *Nuclei in the Cosmos V*, ed. N. Prantzos & S. Harissopoulos, (Paris: Editions Frontières), 216  
 Gallino, R., Busso, M., Picchio, G., & Raiteri, C. M. 1990, *Nature*, 348, 298  
 Gallino, R., Lugaro, M., Busso, M., Arlandini, C., & Straniero, O. 1998b, *Meteoritics Planet. Sci.*, 33, A54  
 Gallino, R., Raiteri, C. M., & Busso, M. 1993, *ApJ*, 410, 400  
 Gallino, R., Raiteri, C. M., Busso, M., & Matteucci, F. 1994, *ApJ*, 430, 858  
 Gao, X., Amari, S., Messenger, S., Nittler, L. R., Swan, P. D., & Walker, R. M. 1996, *Meteoritics & Planet. Sci.*, 31, A48  
 Gao, X., & Nittler, L. R. 1997, *Lunar Planet. Sci.*, 28, 393  
 Gao, X., Nittler, L. R., Swan, P. D., & Walker, R. M. 1995, *Meteoritics*, 30, 508  
 Gilroy, K. K. 1989, *ApJ*, 347, 835  
 Gilroy, K. K. & Brown, J. A. 1991, *ApJ*, 371, 578  
 Heger, A., Langer, N., & Woosley, S.E. 1999, *ApJ*, in press

Henkel, C. & Mauersberg, R. 1993, *A&A*, 274, 730

Herwig, F., Blöcker, T., Schönberner, D., & El Eid, M. 1997, *A&A*, 324, L81

van den Hoek, L. B. & de Jong, T. 1997, *A&A*, 318, 231

Hoppe, P., Amari, S., Zinner, E., Ireland, T., & Lewis, R. S. 1994, *ApJ*, 430, 870

Hoppe, P., Amari, S., Zinner, E., & Lewis, R. S. 1995, *Geochim. Cosmochim. Acta*, 59, 4029

Hoppe, P., Annen, P., Strelbel, R., Eberhardt, P., Gallino, R., Lugaro, M., Amari, S. & Lewis, R. S. 1997, *ApJ*, 487, L101

Hoppe, P., & Ott, U. 1997, in *Astrophysical Implications of the Laboratory Study of Presolar Materials*, ed. T. J. Bernatowicz & E. Zinner (New York: AIP), 27

Hoppe, P., Strelbel, R., Eberhardt, P., Amari, S., & Lewis, R. S. 1996a, *Geochim. Cosmochim. Acta*, 60, 883

Hoppe, P., Strelbel, R., Eberhardt, P., Amari, S., & Lewis, R. S. 1996b, *Science*, 272, 1314

Huss, G. R., Fahey, A. J., Gallino, R., & Wasserburg, G. J. 1994, *ApJ*, 430, L81

Huss, G. R., Fahey, A. J., & Wasserburg, G. J. 1995, *Lunar Planet. Sci.*, 26, 645

Huss, G. R., Hutcheon, I. D., & Wasserburg, G. J. 1997, *Geochim. Cosmochim. Acta*, 61, 5117

Huss, G. R., & Lewis, R. S. 1994a, *Meteoritics*, 28, 791

Huss, G. R., & Lewis, R. S. 1994b, *Meteoritics*, 29, 811

Huss, G. R., & Lewis, R. S. 1995, *Geochim. Cosmochim. Acta*, 59, 115

Hutcheon, I. D., Huss, G. R., Fahey, A. J., & Wasserburg, G. J. 1994, *ApJ*, 425, L97

Iben, I., Jr. 1977a, in *Advanced Stages in Stellar Evolution*, ed. P. Bouvier & A. Maeder (Sauverny: Genève Observatory), 1

Iben, I., Jr. 1977b, *ApJ*, 217, 788

Iben, I. J., & Renzini, A. 1983, *ApJ*, 263, L23

Jones, A., Tielens, A., Hollenbach, D., & McKee, C. 1997, in *Astrophysical Implications of the Laboratory Study of Presolar Materials*, ed. T. Bernatowicz & E. Zinner (New York: AIP), 595

Käppeler, F. 1999, in *Nuclei in the Cosmos V*, ed. N. Prantzos & S. Harissopoulos, (Paris: Editions Frontières), 174

Kehm, K., Amari, S., Hohenberg, C., & Lewis, R. S. 1996, *Lunar Planet. Sci.*, 27, 657

Lambert, D. L., Smith, V. V., Busso, M., Gallino, R., & Straniero, O. 1995, *ApJ*, 450, 302

Langer, N., Heger, A., Wellstein, S., & Herwig, F. 1999a, *A&A*, 346, L37

Langer, N., Heger, A., Woosley, S. E., & Herwig, F. 1999b, in *Nuclei in the Cosmos V*, ed. N. Prantzos & S. Harissopoulos, (Paris: Editions Frontières), 129

Larimer, J. W., & Bartholomay, M. 1979, *Geochim. Cosmochim. Acta*, 43, 1455

Lattanzio, J. C. 1989, *ApJ*, 344, L25

Lattanzio, J. C., & Forestini, M. 1999, in *Asymptotic Giant Branch Stars*, ed. T. Le Bertre, A. Lèbre, & C. Waelkens, IAU Symposium 191, (PASP Conf. Series), 31

Lattanzio, J. C., Frost, C. A., Cannon, R. C., & Wood, P. R. 1997, *Nucl. Phys.*, A621, 435c

Lee, T. 1988, in *Meteorites and the Early Solar System*, ed. J. F. Kerridge & M. S. Matthews (Tucson: University of Arizona Press), 1063

Lewis, R. S., Amari, S., & Anders, E. 1990, *Nature*, 348, 293

Lewis, R. S., Amari, S., & Anders, E. 1994, *Geochim. Cosmochim. Acta*, 58, 471

Lewis, R. S., Tang, M., Wacker, J. F., Anders, E., & Steel, E. 1987, *Nature*, 326, 160

Little-Marenin, I. R. 1986, *ApJ*, 307, L15

Lodders, K., & Fegley Jr., B. 1995, *Meteoritics*, 30, 661

Lodders, K., & Fegley Jr., B. 1997a, *ApJ*, 484, L71

Lodders, K., & Fegley Jr., B. 1997b, in *Astrophysical Implications of the Laboratory Study of Presolar Materials*, ed. T. J. Bernatowicz & E. Zinner (New York: AIP), 391

Lodders, K., & Fegley Jr., B. 1998, *Meteoritics & Planet. Sci.*, 33, 871

Lugaro, M., Gallino, R., Busso, M., Amari, S., & Zinner, E. 1999a, in *Nuclei in the Cosmos V*, ed. N. Prantzos & S. Harissopoulos (Paris: Editions Frontières), 570

Lugaro, M., Gallino, R., Zinner, E., & Amari, S. 1999b, *Lunar Planet. Sci.*, 30, Abstract 1403

Malinie, G., Hartmann, D. H., Clayton, D.D., & Mathews, G. J. 1993, *ApJ*, 413, 633

Martin, P. G., & Rogers, C. 1987, *ApJ*, 322, 374

Mould, J., & Reid, N. 1987, *ApJ*, 321, 156

Nichols, R. H., Jr., Amari, S., Hoppe, P., & Lewis, R. S. 1993, *Meteoritics*, 28, 410

Nichols, R. H., Jr., Hohenberg, C. M., Amari, S., & Lewis, R. S. 1991, *Meteoritics*, 26, 377

Nichols, R. H., Jr., Hohenberg, C. M., Hoppe, P., Amari, S., & Lewis, R. S. 1992, *Lunar Planet. Sci.*, 23, 989

Nichols, R. H., Jr., Kehm, K., Brazzle, R., Amari, S., Hohenberg, C. M., & Lewis, R. S. 1994, *Meteoritics*, 29, 510

Nicolussi, G. K., Davis, A. M., Pellin, M. J., Lewis, R. S., Clayton, R. N., & Amari, S. 1997, *Science*, 277, 1281

Nicolussi, G. K., Pellin, M. J., Lewis, R. S., Davis, A. M., Amari, S., & Clayton, R. N. 1998a, *Geochim. Cosmochim. Acta*, 62, 1093

Nicolussi, G. K., Pellin, M. J., Lewis, R. S., Davis, A. M., Clayton, R. N., & Amari, S. 1998b, *Phys. Rev. Lett.*, 81, 3583

Nicolussi, G. K., Pellin, M. J., Lewis, R. S., Davis, A. M., Clayton, R. N., & Amari, S. 1998c, *ApJ*, 504, 492

Nittler, L. R. 1997, in *Astrophysical Implications of the Laboratory Study of Presolar Materials*, ed. T. J. Bernatowicz & E. Zinner (New York: AIP), 59

Nittler, L. R., & Alexander, C. M. O. D. 1999a, *Lunar Planet. Sci.*, 30, Abstract 2041

Nittler, L. R., & Alexander, C. M. O. D. 1999b, *ApJ*, in press

Nittler, L. R., Alexander, C. M. O. D., Gao, X., Walker, R. M., & Zinner, E. 1994, *Nature*, 370, 443

Nittler, L. R., Alexander, C. M. O. D., Gao, X., Walker, R. M., & Zinner, E. 1997, *ApJ*, 483, 475

Nittler, L. R., Alexander, C. M. O. D., Wang, J., & Gao, X. 1998, *Nature*, 393, 222

Nittler, L. R., et al. 1995, *ApJ*, 453, L25

Nomoto, K., Iwamoto, K., Nakasato, N., Thielemann, F.-K., Brachwitz, F., Tsujimoto, T., Kubo, Y., & Kishimoto, N. 1997, *Nuclear Phys. A*, A621, 467c

Obradovic, M., Brown, L. E., Guha, S., & Clayton, D. D. 1991, *Meteoritics*, 26, 381

Ott, U. 1993, *Nature*, 364, 25

Ott, U., & Begemann, F. 1990a, *ApJ*, 353, L57

Ott, U., & Begemann, F. 1990b, *Lunar Planet. Sci.*, 21, 920

Ott, U., & Begemann, F. 1997, *Meteoritics & Planet. Sci.*, 32, A102

Ott, U., & Begemann, F. 1999, *Meteoritics & Planet. Sci.*, in press

Pellin, M. J., Davis, A. M., Lewis, R. S., Amari, S., & Clayton, R. N. 1999, *Lunar Planet. Sci.*, 30, Abstract 1969

Penzias, A. A. 1981, *ApJ*, 249, 513

Pilachowski, C., Sneden, C., Hinkle, K., & Joyce, R. 1997, *Astron. J.*, 114, 819

Podosek, F. A., Prombo, C. A., Amari, S., & Lewis, R. S. 1999, *ApJ*, in press

Prombo, C. A., Podosek, F. A., Amari, S., & Lewis, R. S. 1993, *ApJ*, 410, 393

Richter, S., Ott, U., & Begemann, F. 1993, in *Nuclei in the Cosmos III*, ed. F. Käppeler & K. Wissak (Bristol and Philadelphia: Institute of Physics Publishing), 127

Richter, S., Ott, U., & Begemann, F. 1994, in *Proc. of the European Workshop on Heavy Element Nucleosynthesis*, ed. E. Somorjai & Z. Fülpö (Debrecen: Inst. Nucl. Res. Hungarian Acad. of Sci.), 44

Schaller, G., Schaerer, D., Meynet, G., & Maeder, A. 1992, *A&AS*, 96, 269

Schatz, H., Jaag, S., Linker, G., Steininger, R., Käppeler, F., Koehler, P. E., Graff, S. M., & Wiescher, M. 1995, *Phys. Rev.*, C51, 379

Secchi, A. 1868, *Mem. Soc. Ital. dei XL*, Ser. III, II, 1

Sharp, C. M., & Wasserburg, G. J. 1995, *Geochim. Cosmochim. Acta*, 59, 1633

Singh, H. P., Roxburgh, I. W., & Chan, K. L. 1998, *A&A*, 340, 178

Smith, V. V., & Lambert, D. L. 1990, *ApJS*, 72, 387

Speck, A. K., Barlow, M. J., & Skinner, C. J. 1997, *MNRAS*, 234, 79

Srinivasan, B., & Anders, E. 1978, *Science*, 201, 51

Stone, J., Hutcheon, I. D., Epstein, S., & Wasserburg, G. J. 1991, *Earth Planet. Sci. Lett.*, 107, 570

Straniero, O., Chieffi, A., Limongi, M., Busso, M., Gallino, R., & Arlandini, C. 1997, *ApJ*, 478, 332

Tang, M., & Anders, E. 1988a, *Geochim. Cosmochim. Acta*, 52, 1235

Tang, M., & Anders, E. 1988b, *ApJ*, 335, L31

Tang, M., Lewis, R. S., Anders, E., Grady, M. M., Wright, I. P., & Pillinger, C. T. 1988, *Geochim. Cosmochim. Acta*, 52, 1221

Thielemann, F.-K., Nomoto, K., & Hashimoto, M.-A. 1996, *ApJ*, 460, 408

Thielemann, F.-K., Nomoto, K., & Yokoi, K. 1986, *A&A*, 158, 17

Timmes, F. X., & Clayton, D. D. 1996, *ApJ*, 472, 723

Timmes, F. X., Woosley, S. E., & Weaver, T. A. 1995, *ApJS*, 98, 617

Travaglio, C., Gallino, R., Amari, S., Zinner, E., Woosley, S., & Lewis, R. S. 1999, *ApJ*, 510, 325

Van Loon, J. T., et al. 1998, *A&A*, 329, 169

Wannier, P.G. 1989, in *The Center of the Galaxy*, ed. M. Morris, IAU Symposium 136 (Dordrecht: Kluwer), 107

Wasserburg, G. J. 1987, *Earth Planet. Sci. Lett.*, 86, 129

Wasserburg, G. J., Boothroyd, A. I., & Sackmann, I.-J. 1995, *ApJ*, 447, L37

Whittet, D. C. B. 1992, *Dust in the Galactic Environment* (New York: Institute of Physics)

Wielen, R., Fuchs, B., & Dettbarn, C. 1996, *A&A*, 314, 438

Wilmes, M. & Köppen, J. 1995, *A&A*, 294, 47

Wissak, K., Guber, K., Voss, F., Käppeler, F., & Reffo, G. 1993, *Phys. Rev.*, C48, 1401

Woosley, S. E. 1996, in *Cosmic Abundances*, ed. S. S. Holt & G. Sonneborn (San Francisco: BookCrafters Inc.), 253

Woosley, S. E., Hoffman, R. D., Timmes, F. X., Weaver, T. A., & Thielemann, F.-K. 1997, *Nucl. Phys.*, A621, 445c

Woosley, S. E., Langer, N., & Weaver, T. A. 1993, *ApJ*, 411, 823

Woosley, S. E., Langer, N., & Weaver, T. A. 1995, *ApJ*, 448, 315

Woosley, S. E., & Weaver, T. A. 1994, *ApJ*, 423, 371

Woosley, S. E., & Weaver, T. A. 1995, *ApJS*, 101, 181

Zinner, E. 1998, *Ann. Rev. Earth Planet. Sci.*, 26, 147

Zinner, E., Amari, S., & Lewis, R. S. 1991, *ApJ*, 382, L47

Zinner, E., Amari, S., Nittler, L. R., Travaglio, C., Gallino, R., Woosley, S., & Lewis, R. S. 1998, *Lunar Planet. Sci.*, 29, Abstract 1763

Zinner, E., Tang, M., & Anders, E. 1989, *Geochim. Cosmochim. Acta*, 53, 3273

## FIGURE CAPTIONS

FIG. 1.— Nitrogen and carbon isotopic ratios measured by secondary ion mass spectrometry in individual presolar SiC grains. Five different classes can be distinguished on the basis of the C, N, and Si isotopic ratios (see also Fig. 2). The abundances of the different classes among all meteoritic SiC are indicated. Note that the numbers of grains of different types in the plot do not correspond to their observed frequencies but that grains from rare classes have been selectively located by ion imaging and are thus over-represented in the graph. Data are from Hoppe et al. (1994, 1996a,b), Nittler et al. (1995), Gao et al. (1996), Amari et al. (1997a,b), and Gao & Nittler (1997).

FIG. 2.— Silicon isotopic ratios measured in individual presolar SiC grains. Isotopic ratios are plotted as  $\delta$ -values, permil ( $\text{‰}$ ) deviations from the solar system ratios:  $\delta^i\text{Si}/^{28}\text{Si} = [(^i\text{Si}/^{28}\text{Si})_{\text{meas}} / (^i\text{Si}/^{28}\text{Si})_{\odot} - 1] \times 1000$ . In this notation the solar ratios have  $\delta$ -values of zero. The same classes as those in Fig. 1 are indicated in the figure. Data are from the same sources as in Fig. 1.

FIG. 3.— Silicon isotopic ratios of “mainstream” SiC grains plotted as  $\delta$ -values from the meteorites Murchison (CM2) and Orgueil (CI). The grain data plot along a line with slope 1.31, which is indicated in the graph. Data are from Hoppe et al. (1994, 1996a) and Huss et al. (1997).

FIG. 4.— The Ti isotopic ratios measured in single mainstream SiC grains from the meteorite Murchison are plotted against their  $^{29}\text{Si}/^{28}\text{Si}$  ratios. The Ti ratios are expressed as  $\delta$ -values as are the Si ratios (see Fig. 2). There is a reasonably good correlation between the Ti ratios, especially the  $^{46}\text{Ti}/^{48}\text{Ti}$  and  $^{47}\text{Ti}/^{48}\text{Ti}$  ratios, and the Si ratios. This indicates that both the Si and Ti isotopic compositions are affected by the same process. Circles are data from Hoppe et al. (1994), squares from Alexander & Nittler (1999).

FIG. 5.— Silicon and Ti isotopic ratios (plotted as  $\delta$ -values) predicted for the envelope of AGB stars of  $1.5$  and  $3 M_{\odot}$  of solar metallicity during dredge-up of material from the He intershell in the TP phase. Solar isotopic ratios were assumed as the starting composition. Small solid symbols indicate that the stars’ envelopes have  $\text{O} > \text{C}$ , large symbols are used when the stars turn into carbon stars ( $\text{C} > \text{O}$ ). Plotted are the results for three different choices of the  $^{13}\text{C}$  pocket, ST indicating the standard case of Gallino et al. (1998), while in the cases d3 and u2 the  $^{13}\text{C}$  mass fraction is one third and twice the amount of the standard case. As can be seen, the Si isotopic ratios are essentially independent of the amount of  $^{13}\text{C}$ , whereas this is not the case for Ti. This means that neutron-capture nucleosynthesis of Si is mostly affected by the  $^{22}\text{Ne}$  and not by the  $^{13}\text{C}$  neutron source. In the Si isotope plot on the upper left the correlation line of the mainstream grains is indicated. A comparison of the predicted Si isotopic ratios with the ratios measured in mainstream grains (Fig. 3) shows that the grain Si data cannot be explained by nucleosynthesis in AGB stars.

FIG. 6.— Titanium isotopic ratios predicted for AGB envelopes of  $1.5$  and  $3 M_{\odot}$  stars of solar metallicity are plotted against the  $^{29}\text{Si}/^{28}\text{Si}$  ratio. All ratios are plotted as  $\delta$ -values. Symbols are the same as those in Fig. 5. A comparison of these graphs with the grain data plotted in Fig. 4 shows that the spread in the Si and Ti isotopic compositions of the grains cannot be explained by nucleosynthesis in AGB stars.

FIG. 7.— Silicon and Ti isotopic ratios predicted for the envelope of a  $5 M_{\odot}$  star of solar metallicity. All ratios are plotted as  $\delta$ -values. Symbols are the same as those in Fig. 5. While the maximum  $\delta^{29}\text{Si}/^{28}\text{Si}$  values reach those observed in mainstream grains (Fig. 3),  $\delta^{30}\text{Si}/^{28}\text{Si}$  values are already  $\sim 120 \text{‰}$  when the star becomes C-rich. Furthermore, the slope of the correlation line of the theoretical ratios is very different from that of the mainstream line plotted in the left upper graph.

FIG. 8.— Silicon and Ti isotopic ratios (plotted as  $\delta$ -values) predicted for the envelope of a  $3 M_{\odot}$  star with lower than-solar metallicity ( $Z=0.006$ ). Symbols are the same as those in Fig. 5. The Si 3-isotope correlation line of the theoretical ratios has a slope of  $\sim 0.5$ , much smaller than that of the mainstream data (upper left graph).

FIG. 9.— Silicon isotopic ratios plotted as  $\delta$ -values of the average ejecta of Type II SN models as function of metallicity. The yields of SNIe of different masses were averaged according to a frequency distribution of  $M^{-2.35}$  per unit mass interval. Silicon yields of Type II SNe of metallicity  $0.1 Z_{\odot}$  and  $Z_{\odot}$  are from WW95, those for  $0.5 Z_{\odot}$  and  $2 Z_{\odot}$  from unpublished data by Weaver & Woosley.

FIG. 10.— Average Si isotopic ratios of the ejecta of Type II SN models of different metallicity (see Fig. 9) are plotted as  $\delta$ -values together with predictions for individual Type II SNe of different masses for the  $0.1 Z_{\odot}$  and the  $Z_{\odot}$  cases (WW95). Also plotted are the predictions of the W7 Type I SN model (Thielemann et al. 1986, Nomoto et al. 1997) and the Type Ia SN model based on a sub-Ch white dwarf (Woosley & Weaver 1994). For a given metallicity there is a large spread in the Si isotopic ratios predicted for stars of different masses. For  $Z=Z_{\odot}$  most stars with  $M < 25 M_{\odot}$  have ratios smaller than the solar ratios whereas stars with  $M \geq 30 M_{\odot}$  have much larger ratios.

FIG. 11.— Silicon isotopic ratios of mainstream grains plotted as  $\delta$ -values and compared with those predicted for the ejecta from the WW95 Type II SN models of solar metallicity. For these models we plotted the predicted values for individual mass stars with  $M \leq 25 M_{\odot}$  (the stars with  $M \geq 30 M_{\odot}$  plot outside of the boundary of the graph) as well as the averages of SNe with  $M \leq 25 M_{\odot}$ , those with  $M \geq 30 M_{\odot}$ , and of all Type II SNe. The  $^{29}\text{Si}$  isotopic yields of all Type II SN models were adjusted (multiplied by a factor of 1.5) so that the  $^{29}\text{Si}/^{30}\text{Si}$  ratio of the average of all SNe is solar (i.e., in the graph the point for the average lies on a straight line through the solar isotopic composition).

FIG. 12.— Silicon isotopic ratios measured in mainstream SiC grains and plotted as  $\delta$ -values (open squares) are compared with the results of Monte Carlo calculations (filled circles) in which contributions from different SN sources are added to a starting isotopic composition in a random way (see text for details). In each case 200 compositions are plotted. (a) Starting composition: average of the mainstream grain ratios. Starting amount:  $1 M_{\odot}$  of material with solar elemental abundances. Contributions from  $N = 100$  SNe were randomly added and subtracted from this starting material. The fraction taken from each SN source was  $a = 1.5 \times 10^{-5}$ . (b) Starting composition is solar;  $N = 70$ ;  $a = 1.7 \times 10^{-5}$ . (c) Starting composition:  $\delta^{29}\text{Si}/^{28}\text{Si} = \delta^{30}\text{Si}/^{28}\text{Si} = -100 \text{‰}$ ;  $N = 420$ ;  $a = 1.1 \times 10^{-5}$ . (d) Starting composition:  $\delta^{29}\text{Si}/^{28}\text{Si} = \delta^{30}\text{Si}/^{28}\text{Si} = -200 \text{‰}$ ;  $N = 600$ ;  $a = 1.5 \times 10^{-5}$ .

FIG. 13.— (a) Elemental ratios calculated from the Monte Carlo model whose Si isotopic ratios are shown in Fig. 12b. The random nature of the SN contributions results not only in a range of Si isotopic compositions but also in a range of elemental ratios. The correspondent  $[\text{Fe}/\text{H}]$  varies from  $\sim 0.06$  to  $\sim 0.1$ . (b) Elemental ratios observed in stars (Edvardsson et al. 1993). We selected only stars with  $-0.1 < [\text{Fe}/\text{H}] < 0.1$ .

FIG. 14.— Silicon isotopic ratios measured in mainstream SiC grains and plotted as  $\delta$ -values (open squares) are compared with the Monte Carlo results shown in Fig. 12c (starting composition  $\delta^{29}\text{Si}/^{28}\text{Si} = \delta^{30}\text{Si}/^{28}\text{Si} = -100 \text{‰}$ ) if the isotopic shift predicted for different AGB models (Figs. 5, 7, and 8) are added. The whole range of shifts predicted under the condition  $\text{C} > \text{O}$  was added in a random way. (a) AGB star of  $1.5 M_{\odot}$  with solar metallicity. (b) AGB star of  $3 M_{\odot}$  with solar metallicity. (c) AGB star of  $5 M_{\odot}$  with solar metallicity. (d) AGB star of  $3 M_{\odot}$  with  $Z=0.006$ .

FIG. 15.— Schematic representation of the Si isotopic ratios of the SiC mainstream grains. (a) If it is assumed that the grains’ parent stars have the same mass and were therefore born at approximately the same time, the spread of the mainstream grain compositions can be interpreted as being due to the heterogeneity of the Si isotopes in the ISM at the formation time of grains’ parent stars. (b) If the grains come from AGB stars with a range of masses, then the spread of the mainstream grain compositions can be interpreted as a superposition of Si isotopic compositions of the ISM at different Galactic ages. In this case, both, isotopic heterogeneity and the Galactic evolution of the Si isotopes contribute to the distribution observed in the grains.

FIG. 16.— Schematic representation of the relative Si isotopic distributions at two different Galactic times. (a) In this case the time difference is  $4.4 \times 10^8$  yr, the evolution time of stars of  $3 M_{\odot}$  mass. The distribution at time  $T_1$  is assumed to be that of the SiC mainstream grains.  $4.4 \times 10^8$  yr later, at the time of solar system formation, the distribution is shifted by  $19 \text{‰}$ . This shift is so small that the actually measured composition of the sun is compatible with the expected spread. (b) For a time difference of  $2.9 \times 10^9$  yr, the evolution time of stars of  $1.5 M_{\odot}$  mass, the predicted isotopic shift ( $125 \text{‰}$ ) is so large, that the sun’s composition is incompatible with the expected spread.

FIG. 17.—In a Si 3-isotope plot the Si isotopic composition of a mixture of two components lies on a straight line connecting these two components. From this it follows that, if we want to reproduce the average isotopic composition of the mainstream SiC grains as a mixture of an arbitrary starting composition (here assumed to be  $\delta^{29}\text{Si}/^{28}\text{Si} = \delta^{30}\text{Si}/^{28}\text{Si} = -100 \text{ ‰}$ ) and the average of all SN contributions, the average SN composition has to lie on a straight line connecting the starting and the average grain compositions. However, the weighted average of all SN sources lies far below this line. An adjustment of the  $^{29}\text{Si}$  yield from SN sources by a factor  $f = 1.5$  is necessary to achieve agreement. Note that the SiC grain average has been corrected for the *s*-process contributions predicted for the AGB parent stars of the grains.

This figure "Figure1.gif" is available in "gif" format from:

<http://arxiv.org/ps/astro-ph/9908055v1>

This figure "Table1.gif" is available in "gif" format from:

<http://arxiv.org/ps/astro-ph/9908055v1>

This figure "Figure2.gif" is available in "gif" format from:

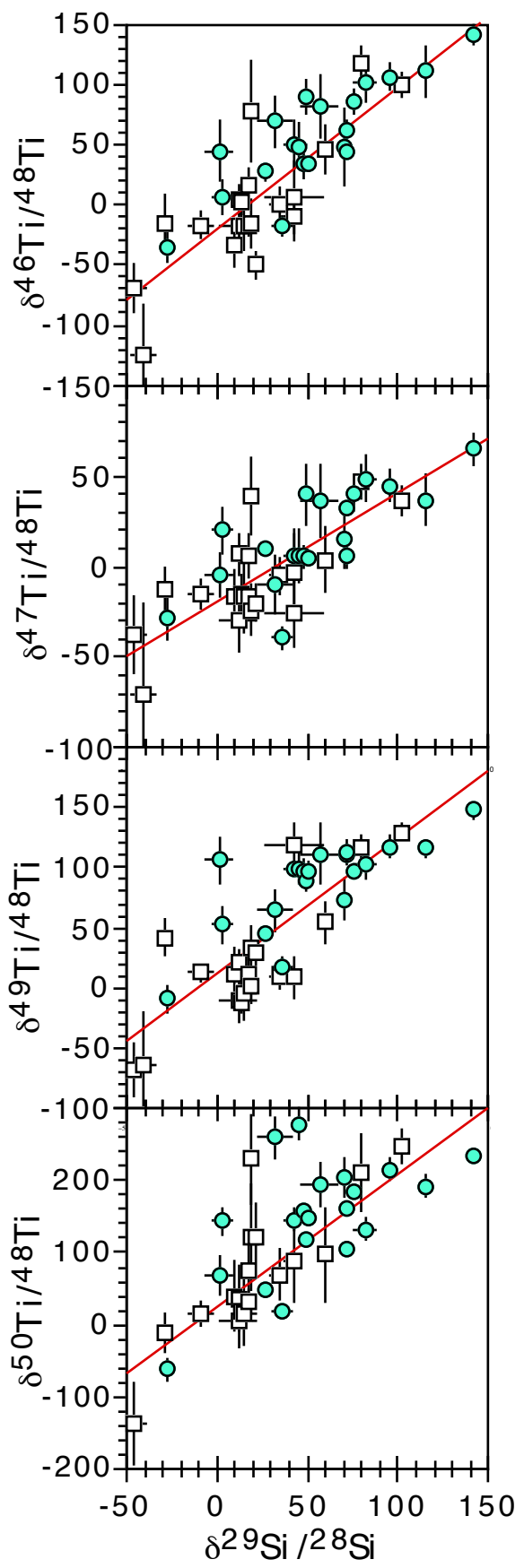
<http://arxiv.org/ps/astro-ph/9908055v1>

This figure "Figure3.gif" is available in "gif" format from:

<http://arxiv.org/ps/astro-ph/9908055v1>

This figure "Table3.gif" is available in "gif" format from:

<http://arxiv.org/ps/astro-ph/9908055v1>



This figure "Table2-4.gif" is available in "gif" format from:

<http://arxiv.org/ps/astro-ph/9908055v1>

This figure "Figure5.gif" is available in "gif" format from:

<http://arxiv.org/ps/astro-ph/9908055v1>

This figure "Figure6.gif" is available in "gif" format from:

<http://arxiv.org/ps/astro-ph/9908055v1>

This figure "Figure7.gif" is available in "gif" format from:

<http://arxiv.org/ps/astro-ph/9908055v1>

This figure "Figure8.gif" is available in "gif" format from:

<http://arxiv.org/ps/astro-ph/9908055v1>

This figure "Figure9.gif" is available in "gif" format from:

<http://arxiv.org/ps/astro-ph/9908055v1>

This figure "Figure10.gif" is available in "gif" format from:

<http://arxiv.org/ps/astro-ph/9908055v1>

This figure "Figure11.gif" is available in "gif" format from:

<http://arxiv.org/ps/astro-ph/9908055v1>

This figure "Figure12.gif" is available in "gif" format from:

<http://arxiv.org/ps/astro-ph/9908055v1>

This figure "Figure13.gif" is available in "gif" format from:

<http://arxiv.org/ps/astro-ph/9908055v1>

This figure "Figure14.gif" is available in "gif" format from:

<http://arxiv.org/ps/astro-ph/9908055v1>

This figure "Figure15.gif" is available in "gif" format from:

<http://arxiv.org/ps/astro-ph/9908055v1>

This figure "Figure16.gif" is available in "gif" format from:

<http://arxiv.org/ps/astro-ph/9908055v1>

This figure "Figure17.gif" is available in "gif" format from:

<http://arxiv.org/ps/astro-ph/9908055v1>